A Finite Element Analysis to Assess the Piezoelectric Non-linearity in Composite Laminated Plate

A Finite Element Analysis to Assess the Piezoelectric Non-linearity in Composite Laminated Plate

Adnan Akhlaq ¹, Mohd Sultan Ibrahim Shaik Dawood ^{1*}, Mohamed Ali Jaffar Syed ¹, Erwin Sulaeman ²

 ¹Department of Mechanical and Aerospace Engineering, Kulliyyah of Engineering, International Islamic University Malaysia, Kuala Lumpur 53100, Malaysia.
 ²Department of Mechanical and Aerospace Engineering, College of Engineering, United Arab Emirates University, Al-Ain P.O. Box 15551, United Arab Emirates.

ABSTRACT

Piezoelectric actuators have been widely used in structural control applications of automotive and aerospace engineering. The numerical and experimental tests show that the linear model applies only to the low electric field where piezoelectric material properties are independent of the electric field whereas at the high electric field the performance of the actuator deviates from the linear model. Investigating the effects of the nonlinear piezoelectric parameters is crucial for the accurate analysis, design, and operation of piezoelectric structures operating under high electric fields. This paper provides a finite element model based on higher-order shear deformation theory to analyse the effect of considering higher-order nonlinear piezoelectric constitutive equations on the static analysis of composite laminated plates at high electric fields. The composite laminated plate bonded with piezoelectric actuators at the top and bottom is used to determine the effect of considering electro-striction and elasto-striction coefficients in the piezoelectric constitutive equation. The applied electric potential in the piezoelectric composite plates is taken to be a linear function across the piezoelectric layer. To determine the non-linear effect in the piezoelectric composite laminated plate under a high electric field, a static analysis is performed by varying the orientation of composite layers and boundary conditions of the plate. The accuracy of the present finite element formulation is validated by comparing it with existing results from the literature. The results of static analysis highlight the importance of considering both higherorder non-linear piezoelectric coefficients in finding the deflection and stresses of composite laminated plates.

Keywords: Elasto-striction, Electro-striction, Composite plate, Piezoelectric structure, Finite element model

I. INTRODUCTION

Application of composite materials is rapidly increasing due to improved stiffness, weight reduction, greater durability, toughness and design flexibility [1-3]. Due to performance characteristics i.e., better stiffness and lightness, laminated composite structures such as composite plates

attracted engineers in the fields of marine, aerospace, automotive, civil, electrical, mechanical and structural engineering [4,5]. Laminated composites are transformed into smart structures by integrating piezoelectric layers, which possess both electrical and mechanical characteristics, enabling them to transform electrical energy into mechanical energy by generating mechanical strain in response to

Manuscript received, September 13, 2024, final revision, March 3, 2025

^{*} To whom correspondence should be addressed, E-mail: sultan@iium.edu.my

Adnan Akhlag

electrical voltage (reverse piezoelectric effect). Conversely, they can also convert mechanical energy into electrical energy by producing charge when subjected to stress (direct piezoelectric effect). Piezoelectric materials having the benefit of electromechanical coupling, rapid response, and high output force can act as actuators and sensors in engineering structures [6,7], which makes them suitable for combining with composite materials. Piezoelectric actuators being inexpensive, compact, and lightweight can be easily shaped and integrated with different surfaces, these special characteristics enable them for application in active noise control and vibration control [8].

Various researchers have conducted static. dynamic and vibration studies of piezoelectric laminated structures considering characteristics of piezoelectric materials where the strain is linearly related to the applied electric field and their material properties are independent of the electric field. However, this is only applicable to homogeneous piezoelectric materials with weak piezoelectric coupling under low electric field applications. Piezoelectric actuators with strong piezoelectric coupling are commonly employed to transmit force at comparatively high electric fields, necessitating the consideration of material nonlinearity in the structural analysis of piezoelectric laminates because of the high electric field [9,10]. Wang et al. [8] experimentally show the non-linear performance of cantilevered uni-morph, bimorph and RAINBOW actuators on applying high electric fields. Masys et al. [11] & Kugel and Cross [12] examined theoretically as well as experimentally the non-linear behavior of piezoelectric ceramics under high sinusoidal electric fields and stress-free conditions. Other works [13-16] have reported similar findings about the non-linear characteristics of piezoelectric materials when high electric field is applied. Yao et al. [17] used classical laminate theory to examine the electro-elastic and electrostrictive properties of cantilever piezoelectric actuators. Thornburgh & Chattopadhyay [18] used refined shear deformation theory to incorporate nonlinear piezoelectric characteristics into the electromechanical model. Wischke et al. [19] calculated the elasto-striction and the electro-striction values of PZT actuators by curve-fitting the experimental results of a cantilevered bimorph.

mathematical derivation based thermodynamic Gibbs potential to incorporate the electro-striction and elasto-striction coefficients in the non-linear constitutive equation is provided by Joshi [20]. Arafa and Baz [21] proposed non-linear piezoelectric characteristics and experimentally investigated the second-order non-linear relationship of piezoelectricity. Tiersten [22] presented non-linear electro-elastic equations that are rotationally invariant for high electric fields with small strain. Chattaraj & Ganguli [23] conducted a non-linear analytical analysis to investigate the electromechanical behavior of a piezoelectric bimorph cantilever under a strong electric field, incorporating second-order constitutive equations for the piezoelectric material. In a subsequent study, Chattaraj & Ganguli [24], extended this non-linear model to examine the response of a piezoelectric bimorph actuator, considering the effect of the selfinduced electric displacement field. They further employed the same non-linear high electric field model to demonstrate the enhanced performance of the piezoelectric bimorph actuator with a tapered geometry [25]. An experimental study was conducted by Ahoor et al. [26] to evaluate the dynamic behavior of a piezoelectric cantilever bimorph, considering material non-linearity.

Liu et al. [27] presented a point interpolation using first order shear deformation theory (FSDT) for static analysis of a piezo-actuated composite laminated plate, considering a linear piezoelectric constitutive model. Phung-Van et al. [28] studied the static and dynamic control of composite laminated piezoelectric structures using the linear constitutive model. On the other hand, Kapuria & Yasin [29] conducted a static analysis of piezo-actuated composite laminates using a layer-wise finite element model considering the non-linear electrostrictive effects under high electric fields and further extended the model to control the vibration of plates and shells [30,31]. Rao et al. [32] performed the static analysis of piezoelectric laminated plates and shells considering the non-linear properties of piezoelectric materials at strong electric field. Zhang et al. [33] developed a geometrically non-linear finite element model including a non-linear piezoelectric constitutive equation when a large electric field is applied to a piezoelectric laminated structure.

The literature review shows that most of the published studies focused on just one type of nonlinearity at high electric fields, i.e., either addressing electro-strictive or elasto-strictive effects, with only a limited number of publications examined the effect of both non-linear electrostriction and elasto-striction coefficients piezoelectric actuators. Recently, Sumit et al. [34-36] performed the static analysis of a piezo-ceramic actuator in bending mode when subjected to a strong electric field using a non-linear constitutive equation and determined the electro-strictive and elastostrictive coefficients for piezo-ceramic by curve fitting the experimental result with analytical derivation. A study of piezoelectric composite laminated beams under strong electric fields using higher order shear deformation theory (HSDT) showing the effects of both non-linear terms was performed by Adnan et al. [37]. The present work addresses the effect of non-linear characteristics, i.e., electro-strictive and elasto-strictive parameters of piezoelectric actuators on the behavior of composite

laminated plates at high electric fields. A finite element model with eight-node quadrilateral elements based on higher-order shear deformation theory is used to perform the static analysis of a piezoelectric composite laminated plate. The present formulation is validated with the existing experimental and numerical results of previous literature.

II. MATHEMATICAL MODELING FOR PIEZOELECTRIC COMPOSITE PLATES

This section presents the mathematical formulation of a piezoelectric composite plate by considering a laminated plate, as shown in Figure 1.

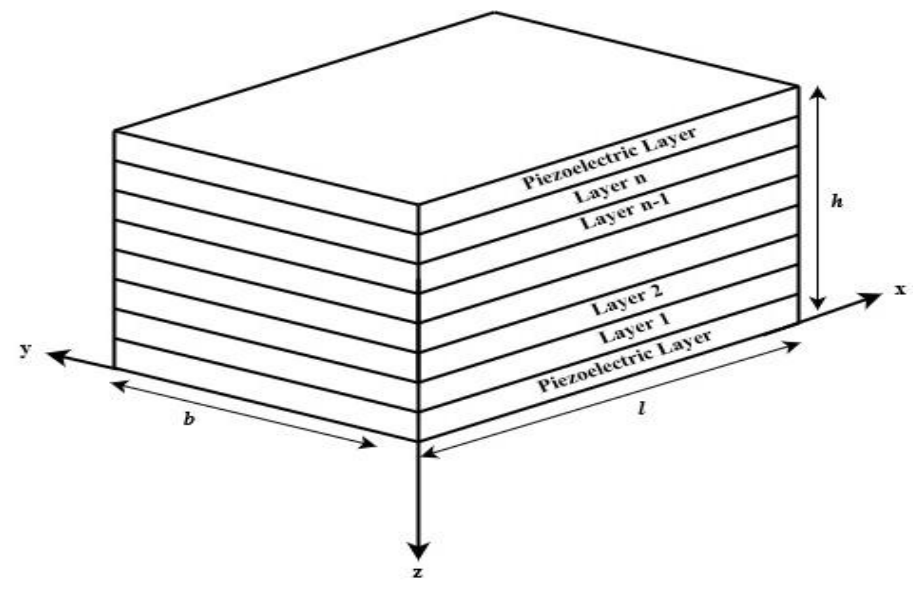


Figure 1 Piezoelectric Composite Laminated Plate with actuator bonded at the top and bottom surface

The laminated plate is assumed to consist of elastic and orthotropic layers with piezoelectric actuators bonded to the top and bottom of the composite laminates, where the electric field acts along the thickness direction of the actuators to enable actuation.

2.1 Non-linear Piezoelectric constitutive equations

Joshi [20] uses the thermodynamic Gibbs potential and the Taylor series expansion up to the second order to calculate the nonlinear strain in piezoelectric actuator:

$$\varepsilon_{ij} = S_{ijlm}^E \sigma_{lm} + d_{ijn} E_n + \frac{1}{2} S_{ijlmpq}^E \sigma_{lm} \sigma_{pq} + \frac{1}{2} d_{ijnr} E_n E_r + \kappa_{ijlmn} \sigma_{lm} E_n$$

$$\tag{1}$$

$$D_k = d_{klm}\sigma_{lm} + \epsilon_{knr}^{\sigma}E_n + \frac{1}{2}\kappa_{klmpq}\sigma_{lm}\sigma_{pq} + \frac{1}{2}\chi_{knr}^{\sigma}E_nE_r + d_{klmn}\sigma_{lm}E_n$$
 (2)

where ε_{ij} and σ_{lm} is the induced strain and the stress in the piezoelectric component, E_n, E_r are the applied electric field, S^E_{ijlm} is the elastic compliance, d_{ijn} and ϵ^{σ}_{knr} is the piezoelectric strain and dielectric constant, S^E_{ijlmpq} is the nonlinear elastic compliance, d_{ijnr} is the electro-

striction coefficient, κ_{ijlmn} is the elasto-striction coefficient and χ^{σ}_{knr} is a non-linear dielectric permittivity coefficient.

The equation for the strain can be given by applying the nonlinear strain expression:

$$\begin{bmatrix} \varepsilon_{xx} \\ \varepsilon_{yy} \\ \gamma_{xy} \end{bmatrix} = \begin{bmatrix} S_{11} & S_{12} & 0 \\ S_{21} & S_{22} & 0 \\ 0 & 0 & S_{66} \end{bmatrix} \begin{bmatrix} \sigma_{xx} \\ \sigma_{yy} \\ \tau_{xy} \end{bmatrix} + \begin{bmatrix} d_{zx} \\ d_{zy} \\ 0 \end{bmatrix} E_z + \frac{1}{2} \begin{bmatrix} d_{zzx} \\ d_{zzy} \\ 0 \end{bmatrix} E_z^2 + \begin{bmatrix} \kappa_{zzx} & 0 & 0 \\ 0 & \kappa_{zzy} & 0 \\ 0 & 0 & 0 \end{bmatrix} \begin{bmatrix} \sigma_{xx} \\ \sigma_{yy} \\ \tau_{xy} \end{bmatrix} E_z$$
 (3)

$$\begin{bmatrix}
D_x \\
D_y \\
D_z
\end{bmatrix} = \begin{bmatrix}
0 & 0 & 0 \\
0 & 0 & 0 \\
d_{zx} & d_{zy} & 0
\end{bmatrix} \begin{bmatrix}
\sigma_{xx} \\
\sigma_{yy} \\
\tau_{xy}
\end{bmatrix} + \begin{bmatrix}
0 \\
0 \\
\varepsilon_{zz}
\end{bmatrix} E_z + \frac{1}{2} \begin{bmatrix}
0 \\
0 \\
0 \\
0 \\
0
\end{bmatrix} E_z^2 + \begin{bmatrix}
0 & 0 & 0 \\
0 & 0 & 0 \\
d_{zzx} & d_{zzy} & 0
\end{bmatrix} \begin{bmatrix}
\sigma_{xx} \\
\sigma_{yy} \\
\tau_{xy}
\end{bmatrix} E_z \tag{4}$$

The non-linear piezoelectric equation can be represented in matrix form as follows:

$$\begin{bmatrix} \varepsilon \\ D \end{bmatrix} = \begin{bmatrix} S & d \\ d & \epsilon \end{bmatrix} \begin{bmatrix} \sigma \\ E \end{bmatrix} \tag{5}$$

$$\begin{bmatrix} \sigma \\ D \end{bmatrix} = \begin{bmatrix} Q & -e \\ e & \epsilon \end{bmatrix} \begin{bmatrix} \varepsilon \\ E \end{bmatrix} \tag{6}$$

Here [S] is the non-linear elastic compliance, [d] is the non-linear piezoelectric strain constant, [O] is the non-linear material stiffness constant, and [e] is the non-linear piezoelectric constant considering non-linear electro and elasto-striction coefficients. These non-linear electrical and mechanical properties of piezoelectric actuators are given by:

$$S_{11} = \frac{1}{E_1}$$
, $S_{12} = \frac{-v_{12}}{E_1}$, $S_{21} = \frac{-v_{21}}{E_2}$, $S_{22} = \frac{1}{E_2}$ and $S_{66} = \frac{1}{G_{12}}$ (5a)

$$S = \begin{bmatrix} S_{11} + \kappa_{zzx} E_z & S_{12} & 0 \\ S_{21} & S_{22} + \kappa_{zzy} E_z & 0 \\ 0 & 0 & S_{66} \end{bmatrix} \text{ and } d = \begin{bmatrix} d_{zx} + \frac{1}{2} d_{zzx} E_z \\ d_{zy} + \frac{1}{2} d_{zzy} E_z \\ 0 \end{bmatrix}$$
 (5b)

$$Q = \begin{bmatrix} Q_{11} & Q_{12} & 0 \\ Q_{21} & Q_{22} & 0 \\ 0 & 0 & Q_{66} \end{bmatrix} \quad \text{and} \quad e = \begin{bmatrix} e_{zx} \\ e_{zy} \\ 0 \end{bmatrix}$$
 (6a)

where
$$e_{zx} = Q_{11} \left(d_{zx} + \frac{1}{2} d_{zzx} E_z \right) + Q_{12} \left(d_{zy} + \frac{1}{2} d_{zzy} E_z \right)$$
 (6b)

and
$$e_{zy} = Q_{21} \left(d_{zx} + \frac{1}{2} d_{zzx} E_z \right) + Q_{22} \left(d_{zy} + \frac{1}{2} d_{zzy} E_z \right)$$
 (6c)

2.2 Displacement field formulation using HSDT

Using the Reddy plate model of higher-order shear deformation theory [38], the displacement

$$u(x, y, z) = u_0(x, y) + z\varphi_x(x, y) - \frac{4z^3}{3h^2}(\varphi_x + \frac{\partial w}{\partial x})$$

$$v(x, y, z) = v_0(x, y) + z\varphi_y(x, y) - \frac{4z^3}{3h^2}(\varphi_y + \frac{\partial w}{\partial y})$$

$$w(x, y, z) = w_0(x, y) \tag{9}$$

where u_0, v_0 and w_0 denotes the mid-plane displacements at any point (x, y, 0). φ_x and φ_y represents the rotation along the x and y axis respectively. In general, the laminate is made up of orthotropic layers, and the transverse shear stresses on the top and bottom layers will be zero. The transverse shear strains and stresses present a quadratic function of the thickness of laminate; therefore, the use of shear correction factors will not be required.

For bending of a 2-D plate the strain components of the plate in terms of displacement field are given as:

field equations for the composite laminated plate through the thickness is given as:

$$\begin{Bmatrix} \varepsilon_{xx} \\ \varepsilon_{yy} \\ \gamma_{xy} \end{Bmatrix} = \begin{Bmatrix} \varepsilon_{xx} \\ \varepsilon_{yy} \\ \varepsilon_{xy} \\ \end{Bmatrix} + z \begin{Bmatrix} \kappa_{xx} \\ \kappa_{yy} \\ \kappa_{xy} \\ \end{Bmatrix} - \frac{4z^3}{3h^2} \begin{Bmatrix} \kappa_{xx}^1 \\ \kappa_{yy}^1 \\ \kappa_{xy}^1 \\ \end{Bmatrix} \tag{10}$$

$$\begin{Bmatrix} \gamma_{yz} \\ \gamma_{xz} \end{Bmatrix} = \begin{Bmatrix} \varepsilon_{yz}^{\circ} \\ \varepsilon_{zx}^{\circ} \end{Bmatrix} - \frac{4z^{2}}{h^{2}} \begin{Bmatrix} \kappa_{yz}^{1} \\ \kappa_{zx}^{1} \end{Bmatrix}$$
(11)

Here, considering $\theta_x = \frac{\partial w}{\partial x}$ and $\theta_y = \frac{\partial w}{\partial y}$

$$\varepsilon_{xx}^{\circ} = \frac{\partial u_o}{\partial x}$$
, $\varepsilon_{yy}^{\circ} = \frac{\partial v_o}{\partial y}$, $\varepsilon_{xy}^{\circ} = \frac{\partial u_o}{\partial y} + \frac{\partial v_o}{\partial x}$ (10a)

$$\varepsilon_{yz}^{\circ} = \frac{\partial w}{\partial y} + \varphi_{y}, \ \varepsilon_{zx}^{\circ} = \frac{\partial w}{\partial x} + \varphi_{x}$$
 (11a)

$$\kappa_{xx}^{\circ} = \frac{\partial \varphi_x}{\partial x}, \quad \kappa_{yy}^{\circ} = \frac{\partial \varphi_y}{\partial y}, \quad \kappa_{xy}^{\circ} = \frac{\partial \varphi_x}{\partial y} + \frac{\partial \varphi_y}{\partial x} \quad (10b)$$

$$\kappa_{xx}^{1} = \frac{\partial \varphi_{x}}{\partial x} + \frac{\partial \theta_{x}}{\partial x}, \quad \kappa_{yy}^{1} = \frac{\partial \varphi_{y}}{\partial y} + \frac{\partial \theta_{y}}{\partial y}, \quad \kappa_{xy}^{1} = \frac{\partial \varphi_{x}}{\partial y} + \frac{\partial \theta_{x}}{\partial y} + \frac{\partial \varphi_{y}}{\partial x} + \frac{\partial \theta_{y}}{\partial x}$$
(10c)

$$\kappa_{vz}^1 = \varphi_v + \theta_v, \quad \kappa_{zx}^1 = \varphi_x + \theta_x \tag{11b}$$

2.3 Energy formulation

In piezoelectric structure, the total strain energy is equivalent to the sum of mechanical strain energy

and the electric field potential energy [39] and is expressed as:

$$U = \frac{1}{2} \int_{v} \sigma \epsilon dv - \frac{1}{2} \int_{v} DE dv$$
 (12)

where ν represents the element volume. Upon substituting Equation (6) into Equation (12), the total strain energy of the piezoelectric structure is expressed as:

$$U = \frac{1}{2} \int_{V} [\sigma \varepsilon - DE] \, dv \tag{13}$$

$$U = \frac{1}{2} \int_{V} [(Q\varepsilon - eE)\varepsilon - (e\varepsilon + \epsilon E)E] dv$$
 (14)

$$U = \frac{1}{2} \int_{v} (Q\varepsilon^{2} - 2eE\varepsilon - \epsilon E^{2}) dv$$
 (15)

An eight-node two-dimensional quadratic quadrilateral iso-parametric element with seven generalized displacement vectors $[u_{oi} \ v_{oi} \ w_i \ \varphi_{xi} \ \varphi_{yi} \ \theta_{xi} \ \theta_{yi}]^T$ is used to discretize the whole plate into a finite number of elements and the nodal displacement vector at each node can be expressed as:

$$\{u^e\} = [u_1 \quad \vdots \quad \cdots \quad \vdots \quad u_8]^T \tag{16}$$

Interpolating the nodal displacement, the generalized displacement vector at any point in terms of shape function can be expressed as:

$$\{u\} = [N] \{u^e\}$$
 (17)

where: [N] = shape function matrix

2.4 Finite Element Formulation

$$[N] = \begin{bmatrix} N_1 & 0 & 0 & 0 & 0 & 0 & \vdots & \dots & \vdots & N_4 & 0 & 0 & 0 & 0 & 0 & 0 \\ 0 & N_1 & 0 & 0 & 0 & 0 & 0 & \vdots & \dots & \vdots & 0 & N_4 & 0 & 0 & 0 & 0 & 0 \\ 0 & 0 & N_1 & 0 & 0 & 0 & 0 & \vdots & \dots & \vdots & 0 & 0 & N_4 & 0 & 0 & 0 & 0 \\ 0 & 0 & 0 & N_1 & 0 & 0 & 0 & \vdots & \dots & \vdots & 0 & 0 & 0 & N_4 & 0 & 0 & 0 \\ 0 & 0 & 0 & 0 & N_1 & 0 & 0 & \vdots & \dots & \vdots & 0 & 0 & 0 & 0 & N_4 & 0 & 0 \\ 0 & 0 & 0 & 0 & 0 & N_1 & 0 & \vdots & \dots & \vdots & 0 & 0 & 0 & 0 & N_4 & 0 & 0 \\ 0 & 0 & 0 & 0 & 0 & N_1 & 0 & \vdots & \dots & \vdots & 0 & 0 & 0 & 0 & N_4 & 0 & 0 \\ 0 & 0 & 0 & 0 & 0 & 0 & N_1 & \vdots & \dots & \vdots & 0 & 0 & 0 & 0 & 0 & N_4 & 0 \\ 0 & 0 & 0 & 0 & 0 & 0 & N_1 & \vdots & \dots & \vdots & 0 & 0 & 0 & 0 & 0 & N_4 & 0 \\ 0 & 0 & 0 & 0 & 0 & 0 & N_1 & \vdots & \dots & \vdots & 0 & 0 & 0 & 0 & 0 & N_4 & 0 \\ \end{bmatrix}$$

The strain $\{\varepsilon_b\}$ associated with the element is written as:

$$\begin{Bmatrix} \varepsilon_{xx} \\ \varepsilon_{yy} \\ \gamma_{xy} \end{Bmatrix} = [Z_b'] \{\bar{\varepsilon}_b\} \{u\} = [N] \{u^e\}$$
(18)

where:

$$\{\bar{\varepsilon}_b\} = [\varepsilon_{xx}^{\circ} \quad \varepsilon_{yy}^{\circ} \quad \varepsilon_{xy}^{\circ} \quad \kappa_{xx}^{\circ} \quad \kappa_{yy}^{\circ} \quad \kappa_{xy}^{\circ} \quad \kappa_{xx}^{1} \quad \kappa_{yy}^{1} \quad \kappa_{xy}^{1}]^T$$
(18a)

$$[Z_{b}'] = \begin{bmatrix} 1 & 0 & 0 & z & 0 & 0 & -c_{1}z^{3} & 0 & 0 \\ 0 & 1 & 0 & 0 & z & 0 & 0 & -c_{1}z^{3} & 0 \\ 0 & 0 & 1 & 0 & 0 & z & 0 & 0 & -c_{1}z^{3} \end{bmatrix}$$
(18b)

The generalized strain $\{\bar{\varepsilon}_b\}$ at any point in the $\{\bar{\varepsilon}_b\} = [B_b]\{u^e\}$ (19) element can be expressed as:

where

$$\{B_b\} = \begin{bmatrix} \frac{\partial N_1}{\partial x} & 0 & 0 & 0 & 0 & 0 & \vdots & \cdots & \vdots & \frac{\partial N_8}{\partial x} & 0 & 0 & 0 & 0 & 0 & 0 \\ 0 & \frac{\partial N_1}{\partial y} & 0 & 0 & 0 & 0 & 0 & \vdots & \cdots & \vdots & 0 & \frac{\partial N_8}{\partial y} & 0 & 0 & 0 & 0 & 0 \\ \frac{\partial N_1}{\partial y} & \frac{\partial N_1}{\partial x} & 0 & 0 & 0 & 0 & \vdots & \cdots & \vdots & \frac{\partial N_8}{\partial y} & \frac{\partial N_8}{\partial x} & 0 & 0 & 0 & 0 & 0 \\ 0 & 0 & 0 & \frac{\partial N_1}{\partial x} & 0 & 0 & 0 & \vdots & \cdots & \vdots & 0 & 0 & 0 & \frac{\partial N_8}{\partial x} & 0 & 0 & 0 \\ 0 & 0 & 0 & \frac{\partial N_1}{\partial y} & 0 & 0 & \vdots & \cdots & \vdots & 0 & 0 & 0 & \frac{\partial N_8}{\partial x} & 0 & 0 & 0 \\ 0 & 0 & 0 & \frac{\partial N_1}{\partial y} & \frac{\partial N_1}{\partial x} & 0 & 0 & \vdots & \cdots & \vdots & 0 & 0 & 0 & \frac{\partial N_8}{\partial y} & \frac{\partial N_8}{\partial x} & 0 & 0 \\ 0 & 0 & 0 & \frac{\partial N_1}{\partial x} & 0 & \frac{\partial N_1}{\partial x} & 0 & \vdots & \cdots & \vdots & 0 & 0 & 0 & \frac{\partial N_8}{\partial y} & \frac{\partial N_8}{\partial x} & 0 \\ 0 & 0 & 0 & \frac{\partial N_1}{\partial x} & 0 & \frac{\partial N_1}{\partial y} & \vdots & \cdots & \vdots & 0 & 0 & 0 & \frac{\partial N_8}{\partial y} & \frac{\partial N_8}{\partial x} & \frac{\partial N_8}{\partial y} & \frac{\partial N_8}{\partial x} \\ 0 & 0 & 0 & \frac{\partial N_1}{\partial y} & \frac{\partial N_1}{\partial y} & \frac{\partial N_1}{\partial y} & \vdots & \cdots & \vdots & 0 & 0 & 0 & \frac{\partial N_8}{\partial y} & \frac{\partial N_8}{\partial x} & \frac{\partial N_8}{\partial y} & \frac{\partial N_8}{\partial x} \\ 0 & 0 & 0 & \frac{\partial N_1}{\partial y} & \frac{\partial N_1}{\partial y} & \frac{\partial N_1}{\partial y} & \vdots & \cdots & \vdots & 0 & 0 & 0 & \frac{\partial N_8}{\partial y} & \frac{\partial N_8}{\partial x} & \frac{\partial N_8}{\partial y} & \frac{\partial N_8}{\partial x} \\ 0 & 0 & 0 & \frac{\partial N_1}{\partial y} & \frac{\partial N_1}{\partial y} & \frac{\partial N_1}{\partial y} & \frac{\partial N_1}{\partial y} & \vdots & \cdots & \vdots & 0 & 0 & 0 & \frac{\partial N_8}{\partial y} & \frac{\partial N_8}{\partial x} & \frac{\partial N_8}{\partial y} & \frac{\partial N_8}{\partial x} \\ 0 & 0 & 0 & \frac{\partial N_1}{\partial y} & \frac{\partial N_1}{\partial y} & \frac{\partial N_1}{\partial y} & \frac{\partial N_1}{\partial y} & \vdots & \cdots & \vdots & 0 & 0 & 0 & \frac{\partial N_8}{\partial y} & \frac{\partial N_8}{\partial y} & \frac{\partial N_8}{\partial y} & \frac{\partial N_8}{\partial x} \\ 0 & 0 & 0 & \frac{\partial N_1}{\partial y} & \frac{\partial N_1}{\partial y} & \frac{\partial N_1}{\partial y} & \frac{\partial N_1}{\partial y} & \vdots & \cdots & \vdots & 0 & 0 & 0 & \frac{\partial N_8}{\partial y} & \frac{\partial N_8}{\partial y} & \frac{\partial N_8}{\partial y} & \frac{\partial N_8}{\partial y} \\ 0 & 0 & 0 & \frac{\partial N_1}{\partial y} & \frac{\partial N_1}{\partial y} & \frac{\partial N_1}{\partial y} & \frac{\partial N_1}{\partial y} & \vdots & \cdots & \vdots & 0 & 0 & 0 & \frac{\partial N_8}{\partial y} & \frac{\partial N_8}{\partial y} & \frac{\partial N_8}{\partial y} & \frac{\partial N_8}{\partial y} \\ 0 & 0 & 0 & \frac{\partial N_1}{\partial y} & \frac{\partial N_1}{\partial y} & \frac{\partial N_1}{\partial y} & \frac{\partial N_1}{\partial y} & \vdots & \cdots & \vdots & 0 & 0 & 0 & \frac{\partial N_8}{\partial y} & \frac{\partial N_8}{\partial y} & \frac{\partial N_8}{\partial y} & \frac{\partial N_8}{\partial y} \\ 0 & 0 & 0 & 0 & \frac{\partial N_1}{\partial y} & \frac{\partial N_1}{\partial y} & \frac{\partial N_1}{\partial y} & \frac{\partial N_1}{\partial y} & \vdots$$

The transverse shear strain $\{\varepsilon_s\}$ associated with the element is written as:

Adnan Akhlag

$${\gamma_{yz} \brace \gamma_{xz}} = [Z_s] \{\bar{\varepsilon}_b\}$$
 (20)

where

$$\{\bar{\varepsilon}_B\} = \begin{bmatrix} \varepsilon_{zx}^{\circ} & \varepsilon_{yz}^{\circ} & \kappa_{zx}^{1} & \kappa_{yz}^{1} \end{bmatrix}^T$$
 (20a)

$$[Z_{s'}] = \begin{bmatrix} 0 & 1 & 0 & -c_2 z^2 \\ 1 & 0 & -c_2 z^2 & 0 \end{bmatrix}$$
 (20b)

The generalized strain $\{\bar{\varepsilon}_s\}$ at any point in the element can be expressed as:

$$\{\bar{\varepsilon}_{s}\} = [B_{s}]\{u^{e}\} \tag{21}$$

where:

$$\{B_s\} = \begin{bmatrix} 0 & 0 & \frac{\partial N_1}{\partial x} & N_1 & 0 & 0 & 0 & \vdots & \cdots & \vdots & 0 & 0 & \frac{\partial N_8}{\partial x} & N_8 & 0 & 0 & 0 \\ 0 & 0 & \frac{\partial N_1}{\partial y} & 0 & N_1 & 0 & 0 & \vdots & \cdots & \vdots & 0 & 0 & \frac{\partial N_8}{\partial y} & 0 & N_8 & 0 & 0 \\ 0 & 0 & 0 & N_1 & 0 & N_1 & 0 & \vdots & \cdots & \vdots & 0 & 0 & 0 & N_8 & 0 & N_8 & 0 \\ 0 & 0 & 0 & 0 & N_1 & 0 & N_1 & \vdots & \cdots & \vdots & 0 & 0 & 0 & 0 & N_8 & 0 & N_8 \end{bmatrix}$$
 (21a)

As a linearly varying electric potential is applied along the thickness of the piezoelectric layer, the electric field can be given in matrix form as:

$$\{E\} = \begin{bmatrix} 0\\0\\-\frac{\emptyset}{t} \end{bmatrix} \tag{22}$$

$$\{E\} = [B_{\emptyset}][\emptyset] \tag{23}$$

where

$$[B_{\emptyset}] = \begin{bmatrix} 0 \\ 0 \\ -\frac{1}{t} \end{bmatrix} \tag{24}$$

$$[K^e]_b = \int_{-1}^1 \int_{-1}^1 [B_b]^T (\int [Z_b{'}]^T \overline{Q_b} [Z_b{'}] dz) [B_b] det J d\zeta d\eta$$

$$[K^e]_S = \int_{-1}^1 \int_{-1}^1 [B_S]^T (\int [Z_S]^T \overline{Q_S}[Z_S]^T dz) [B_S] det J d\zeta d\eta$$

$$[K^{e}]_{\emptyset} = \int_{-1}^{1} \int_{-1}^{1} [B_{b}]^{T} (\int [Z_{b}']^{T} [e] dz) [B_{\emptyset}] det J d\zeta d\eta$$

$$[f^e] = \int_{-1}^{1} \int_{-1}^{1} [N]^T q \, det J d\zeta d\eta \tag{30}$$

The global stiffness matrix will be formed by meshing the elemental stiffness matrices, considering seven mechanical and one electrical degrees of freedom. The equation of motion is expressed in terms of the global stiffness matrix as follows:

$$\{ [K]_b + [K]_s \} [w] - [K]_{\emptyset} [\emptyset] = [f]$$
(31)

where $[K]_b$, $[K]_s$, $[K]_\emptyset$ and [f] are global stiffness matrices for bending, shear electrical and mechanical load respectively. The deflection at each node can be solved by using Equation (31) which

2.5 Principle of Virtual Work The stiffness matrices are obtained by applying the principle of minimum potential energy using the principle of virtual work for piezoelectric plates with the total potential energy is expressed as:

$$\prod = \sum U - \sum f u_e - \int_{\mathcal{A}} \phi Q dA \tag{25}$$

The total potential energy is minimum when its first variation is equal to zero in terms of nodal displacement.

$$\frac{\partial \Pi}{\partial u_e} = \frac{\partial}{\partial u_e} \sum U - \frac{\partial}{\partial u_e} \sum f u_e = 0 \tag{26}$$

The stiffness matrices for bending, shearing, electrical and uniformly distributed load are obtained after solving this equation:

can be further used for stress analysis of piezoelectric laminated plate.

III. RESULTS AND DISCUSSION

3.1 Validation of the present model with cantilever and simply supported plate with linear piezoelectric constitutive relation

The present finite element model with linear constitutive equation is validated by considering a cantilevered composite laminated plate analyzed using FSDT [27] and CLT [40]. The square plate with length and width of 20 cm, consists of T300/976 graphite-epoxy composite layers stacked in the sequence $(p/-45^{\circ}/45^{\circ}/-45^{\circ}/45^{\circ}/p)$, and has symmetrically bonded piezoelectric ceramics

(PZT G-1195) on its upper and lower surfaces. The composite plate has a total thickness of 1 mm, with each piezo-layer having a thickness of 0.1 mm. The plate is discretized using 8-node quadratic quadrilateral iso- parametric elements, as shown in Figure 2, with a mesh consisting of 400 elements arranged in a 20×20 configuration for numerical analysis.

The material properties used in the analysis are listed in Table 1. When an electric potential of 10 V is applied through the distributed actuators, the centre-line deflection is computed and presented in Figure 3, to demonstrate the accuracy of the linear model. Figure 4 presents the variation of deflection at the centre-line free end as the electric potential increases from 0 to 60 V. The plot of the centre-line deflection of the plate against the input voltage of the actuator is found to have a linear relationship as

the deflection is calculated using a linear piezoelectric constitutive equation.

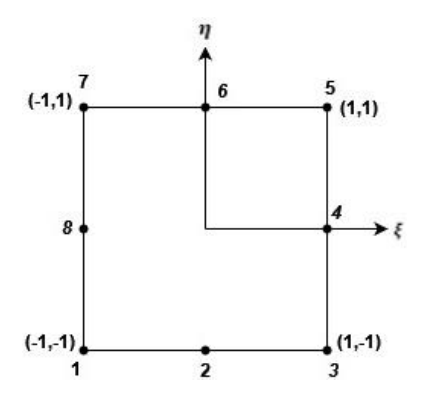


Figure 2 Eight-node quadratic element with Jacobian coordinates

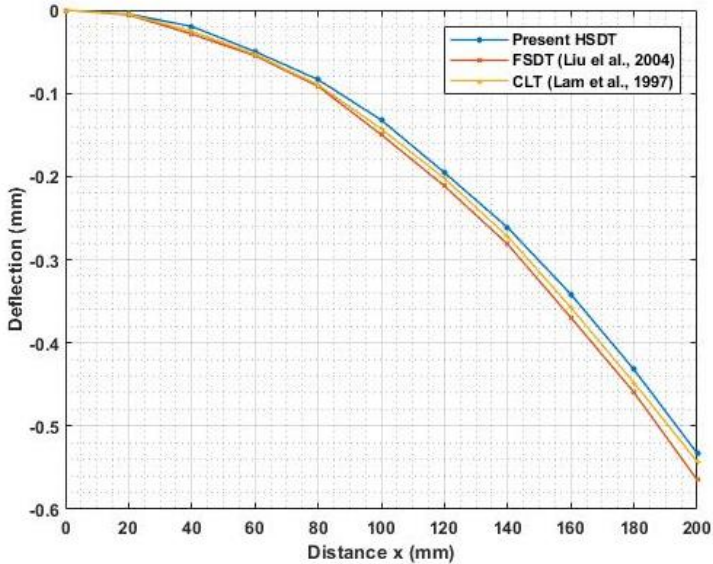


Figure 3 Centreline deflection of cantilever plate on applying 10 V electric potential

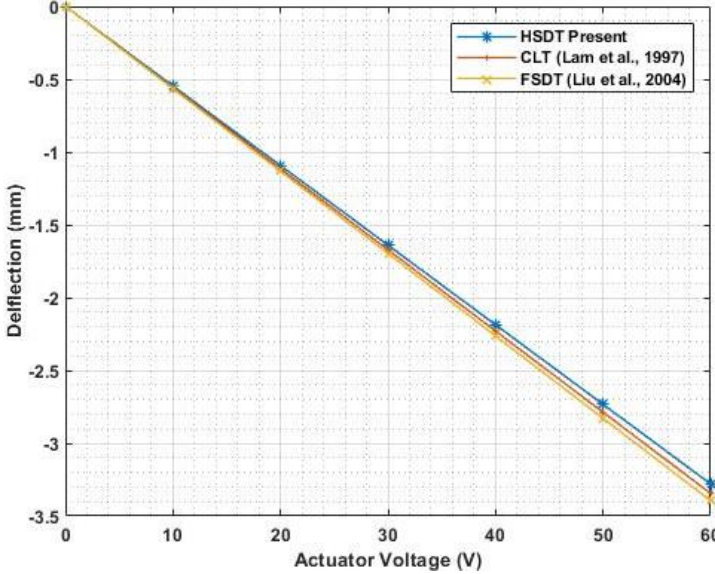


Figure 4 Variation of centre-line free end deflection against actuator input voltage

Adnan Akhlaq

To further validate the linear constitutive model a simply-supported laminated composite plate made of graphite-epoxy (T300/976), actuated by PZT (G-1195) piezoceramic [27,28] is considered. The material properties are listed in Table 1 and the plate has dimensions of 20 cm \times 20 cm , with piezoelectric material bonded to the top and bottom surfaces, where each piezoelectric layer has a thickness of 0.1 mm, and each composite layer is 0.25 mm thick. The laminated plate is subjected to a uniform load of $q = 100 \ N/m^2$ along with

varying input voltages of 0V, 5V and 10V. The centerline deflections for symmetric and antisymmetric plates with fibre orientations of $(p/-15/15)_{as}$, $(p/-30/30)_{as}$, $(p/-45/45)_{as}$ and $(p/-45/45)_{s}$ are shown in Figure 5, while the deflection at the mid-point of the simply supported plate is presented in Table 2. The deflection values obtained using the current model presented here match well with the previously published results with errors being less than 5%.

Table 1 Material properties (E_i , G_{ij} in GPa and d_{ij} in 10^{-12} mV^{-1})

Material	E_1	$\boldsymbol{E_2}$	E_3	G ₂₃	G ₁₃	G ₁₂	v_{23}	v_{13}	v_{12}	
PZT 3203 HD [8]	60.24	60.24	47.619	19.084	19.084	24.04	0.494	0.494	0.253	
PZT G1195N [29]	63	63	63	24.2	24.2	24.2	0.3	0.3	0.3	
T300/976 [29]	150	9	9	2.5	7.1	7.1	0.3	0.3	0.3	
PZT APC 850 [34]	63	63	63	24.05	24.05	24.05	0.31	0.31	0.31	
Al [29]	70	70	70	26.92	26.92	26.92	0.3	0.3	0.3	
Silicon [34]	166	166	166	65.9	65.9	65.9	0.26	0.26	0.26	
	d_{31}	d ₃₂	d ₃₃	$d_{331} (m^2 V^{-2})$		$\kappa_{331} (m^3 N^{-1} V^{-1})$				
PZT 3203 HD [8]	-320	-320	-	-520×10^{-18}		-				
PZT G1195N [29]	-254	-254	-	-165×10^{-18}		-				
PZT APC 850 [34]	-175	-175	-	-1210×10^{-18}			-6.3×10^{-17}			

Table 2 Central node deflections of the simply supported laminate under uniform loading and different actuator input loads $(\times 10^{-4} m)$

Input Voltage	Layer scheme	Liu et al. [27]	Present	error (%)
0	$(p/-45/45)_s$	-0.6038	-0.62965	4.281219
0	$(p/-45/45)_{as}$	-0.6217	-0.6462	3.940807
0	$(p/-30/30)_{as}$	-0.6542	-0.6809	4.081321
0	$(p/-15/15)_{as}$	-0.7222	-0.7535	4.33398
5	$(p/-45/45)_s$	-0.2717	-0.28413	4.574899
5	$(p/-45/45)_{as}$	-0.273	-0.2835	3.846154
5	$(p/-30/30)_{as}$	-0.2862	-0.29794	4.102027
5	$(p/-15/15)_{as}$	-0.3134	-0.3282	4.722399
10	$(p/-45/45)_s$	0.0604	0.06314	4.536424
10	$(p/-45/45)_{as}$	0.0757	0.07925	4.689564
10	$(p/-30/30)_{as}$	0.0819	0.08503	3.821734
10	$(p/-15/15)_{as}$	0.0954	0.09728	1.97065

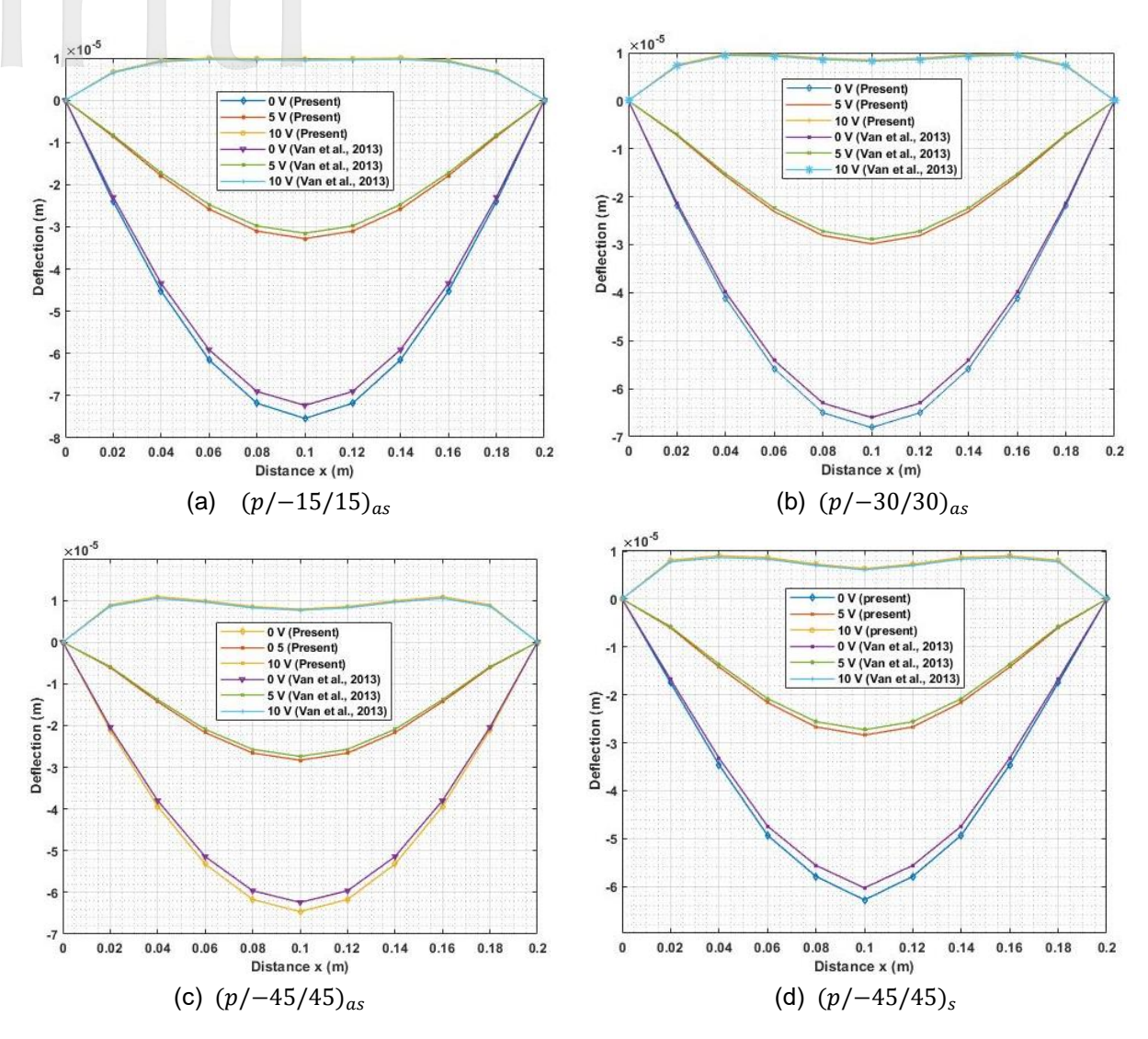


Figure 5 Centerline deflections of the simply supported laminates under uniform loading and different actuator input voltages

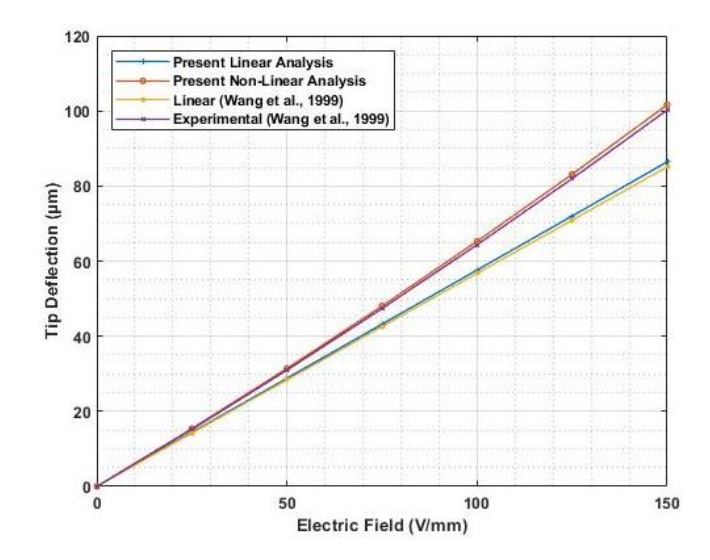


Figure 6 Variation of tip deflection of cantilever bimorph beam against the applied electric field.

3.2 Validation of the present Non-linear model using simply supported bimorph plate and cantilever uni-morph

The effect of the electro-strictive coefficient on beam deflection is validated using the cantilever bimorph experimentally analyzed by Wang et al. [8]. It consists of a soft PZT (3203 HD) with two actuator layers, each having a thickness of 0.5 mm and dimensions of 35 × 7 mm, actuated with opposite polarity. The linear and nonlinear properties of PZT (3203 HD) are provided in Table 1 and the comparison of linear and non-linear tip deflections against varying electric fields, with the experimental results from Wang et al. [8] is presented in Figure 6. The analysis is performed using the current finite element formulation, which employs a 20 × 20 element mesh with 8-node quadratic quadrilateral iso-parametric elements. The results demonstrate that the predictions from the present non-linear model agree well with the experimental measurements. Furthermore, the tip deflection obtained using the non-linear constitutive equation shows a significant deviation from the linear predictions at higher actuation fields highlighting the importance of accounting for nonlinear effects.

Erwin Sulaeman

Considering the effect of the non-linear electrostriction coefficient at a large electric field, a simply supported plate composed of aluminium substrate with PZT (G-1195) piezoceramic layers bonded to its top and bottom surfaces was studied by Kapuria & Yasin [29] and Yao et al. [41]. The plate has a length and width of 40 mm, with a total thickness of 0.75 mm. The deflection at the midpoint of the cantilever plate, calculated using the formulation for both linear and non-linear piezoelectric constitutive relations is presented in Figure 7. The results show good agreement with previously published data.

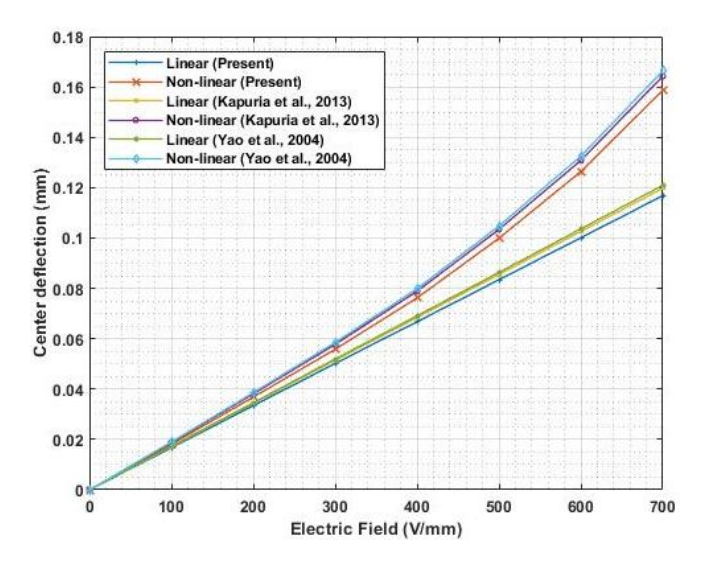


Figure 7 Variation of mid-point deflection of simply supported bimorph plate with aluminium substrate

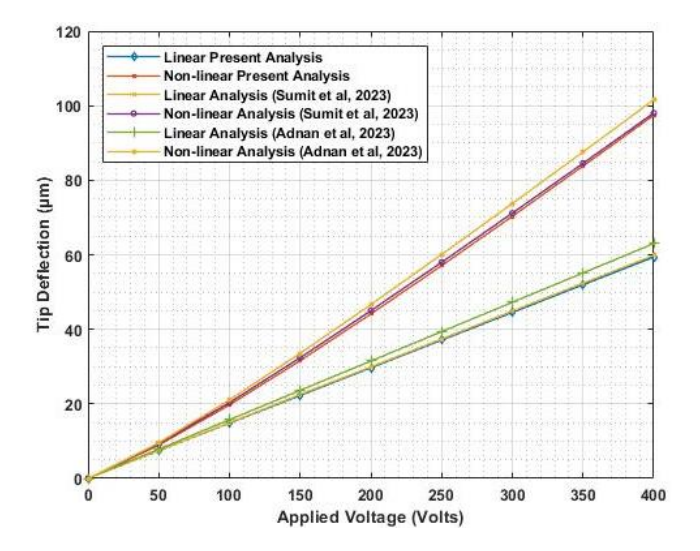


Figure 8 Variation of tip deflection of cantilever uni-morph plate with increasing electric potential.

To validate the non-linear effects of both electro-strictive and elasto-strictive coefficients under high electric fields, a PZT (APC 850) cantilever uni-morph beam with dimensions of 23 × 3 mm is considered. The piezoelectric actuator has a thickness of 0.3 mm and is bonded to a 0.675 mm thick silicon elastic layer. The material properties of the cantilever uni-morph are provided in Table 1. Figure 8 presents the tip deflection results based on both linear and non-linear piezoelectric equations, with the results showing good agreement with the findings of Sumit et al. [34] and Adnan et al. [37].

3.3 Non-linear Analysis of piezoelectric composite laminated plate

The effect of elasto-striction and electrostriction non-linear parameters is investigated using symmetric cross-ply and anti-symmetric angle-ply composite laminated plates with different end conditions.

A simply supported square laminated composite plate with symmetric cross-ply and antisymmetric angle-ply configurations is considered. The laminate consists of four layers of graphite-epoxy substrate bonded to two outer layers of PZT APC (850) piezoceramic material, with corresponding material properties provided in Table 1. The plate has a span length of 200 mm and a thickness ratio of l/h = 10. The thickness of each

non-piezoelectric composite layer is 0.2 h and the thickness of each piezo-layer is 0.1 h. The fiber considered $(p/-45^{\circ}/$ orientations are $(45^\circ)_{as}$ and $(p/0^\circ/90^\circ)_s$. The plate is modeled using 8-node iso-parametric quadratic finite elements based on higher-order shear deformation theory. A convergence test is performed to determine the minimum number of elements required to accurately predict the behavior of the composite laminate under piezoelectric actuation. The results of the transverse deflection of the composite laminated plate are presented in Figure 9, which demonstrates that the transverse deflection converges for both antisymmetric angle-ply and symmetric cross-ply configurations after using 400 elements, corresponding to a mesh size of 20 × 20.

When an increasing electric field from 0 to 700 V/mm is applied across the simply supported antisymmetric angle-ply composite laminate, the variations of linear and non-linear central deflection, normal stress in both the piezoelectric and composite layers, as well as in-plane shear stress at the top of the piezoelectric layer are presented in Figure 10. The results are presented by considering the electro-striction coefficient alone, the elasto-striction coefficient alone, and both the non-linear terms.

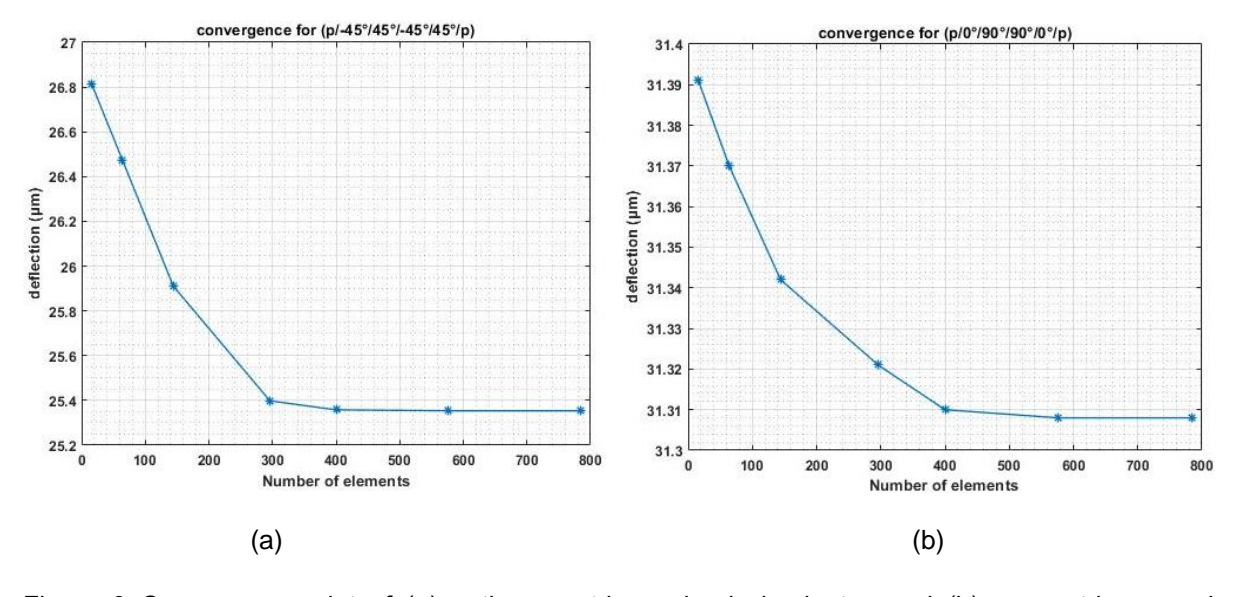


Figure 9 Convergence plot of (a) anti-symmetric angle-ply laminates and (b) symmetric coss-ply laminates

The effect of elasto-striction is more dominant in the normal stress of the piezoelectric layer than in the deflection, normal stress and in-plane shear stress in the composite layer, due to the reduction in elastic property of the PZT layer. Moreover, applying a positive electric field reduces the elastic properties of the piezoelectric material, due to elasto-striction term, which results in a decrease in

deflection and stresses. Equation (6) shows that the elastic properties increase with the application of an increasing negative electric field, resulting in higher deflection and stress values, highlighting the need to include higher-order non-linear piezoelectric terms for an improved and more accurate static response. The elastic property may increase or decrease with the application of a negative or positive electric field

however, the effective piezoelectric strain coefficient increases with a positive or negative electric field, as explained by Kapuria & Yasin [29] and given by $d_{zx}^e = d_{zx} + \frac{1}{2}d_{zzx}|E_z|$. As the strain

produced in the piezoelectric layer is quadratic variation of the electric field, therefore the absolute value of the electric field is considered.

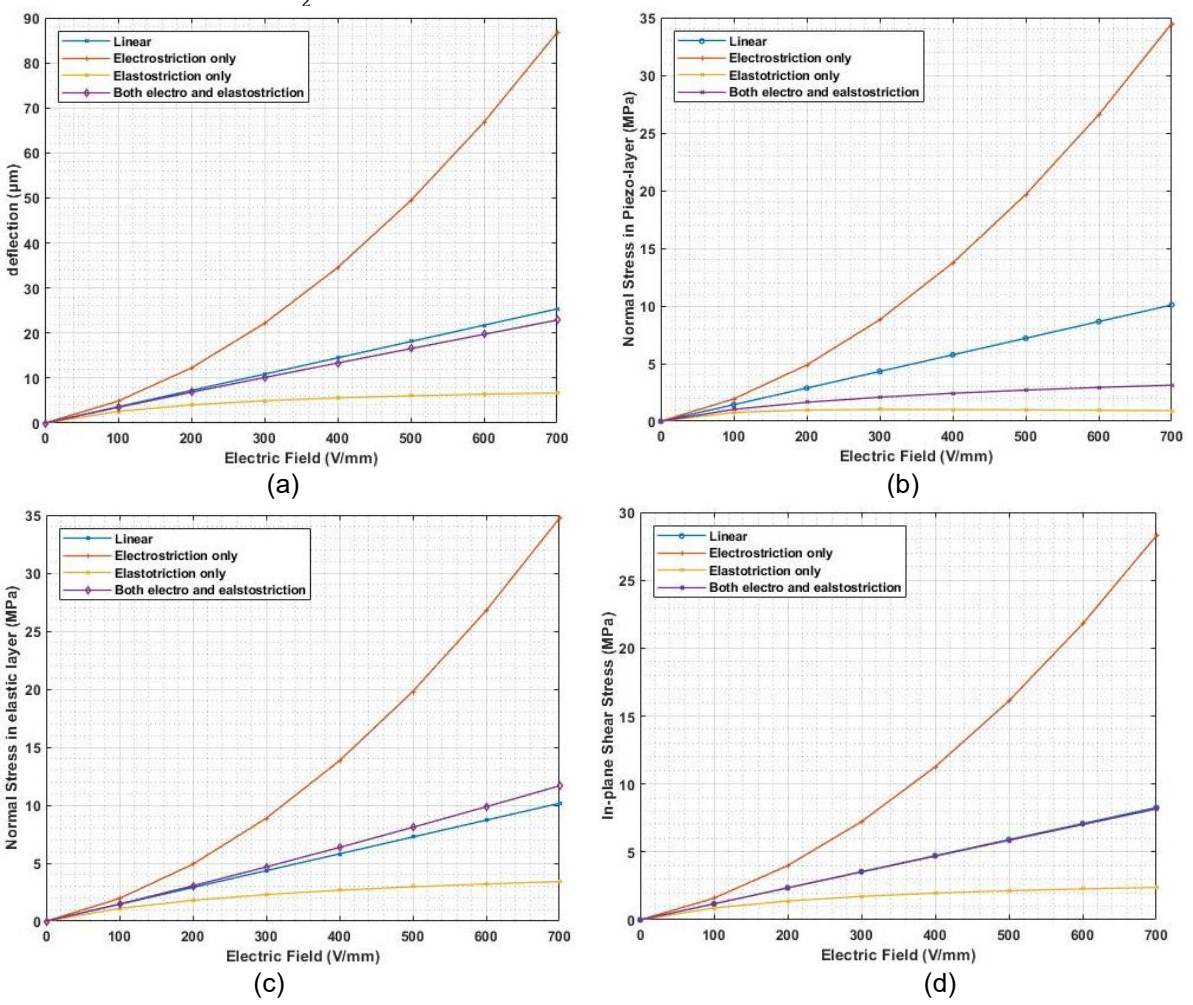
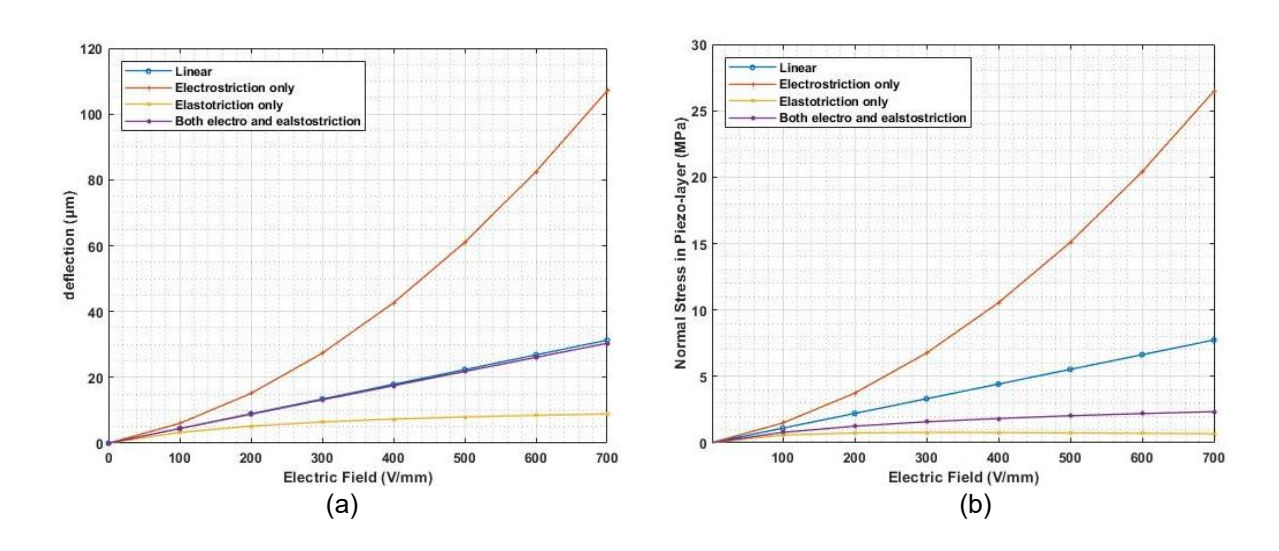


Figure 10 Variation of (a) central deflection, (b) Normal stress in piezo-layer σ^p_{xx} (0.5a, 0.5b, 0.5h), (c) Normal stress in the composite layer σ^e_{xx} (0.5a, 0.5b, 0.4h) and (d) In-plane shear stress at the top layer τ_{xy} (a, 0.5b, 0.5h) for anti-symmetric angle-ply laminates



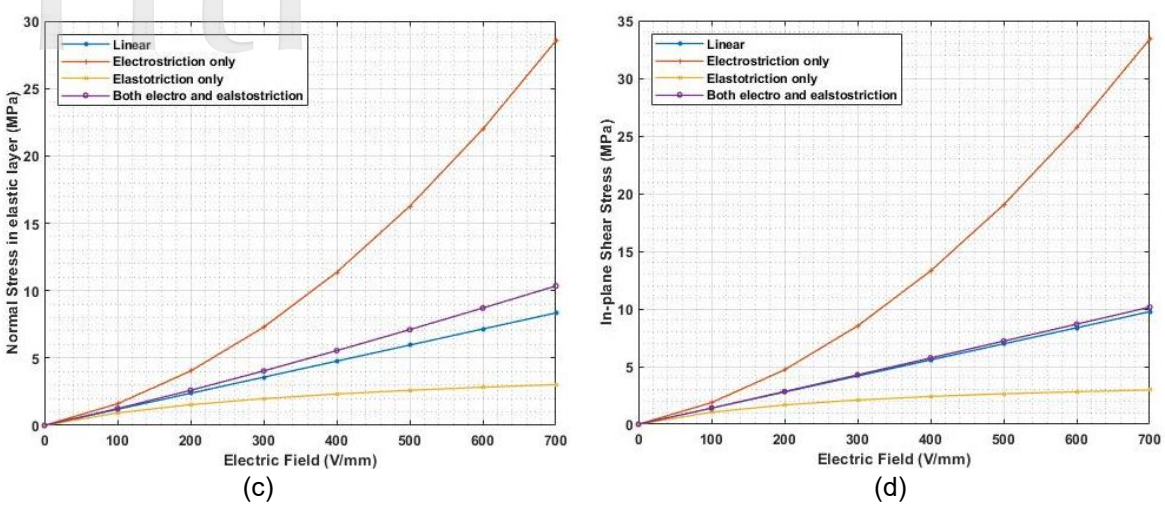


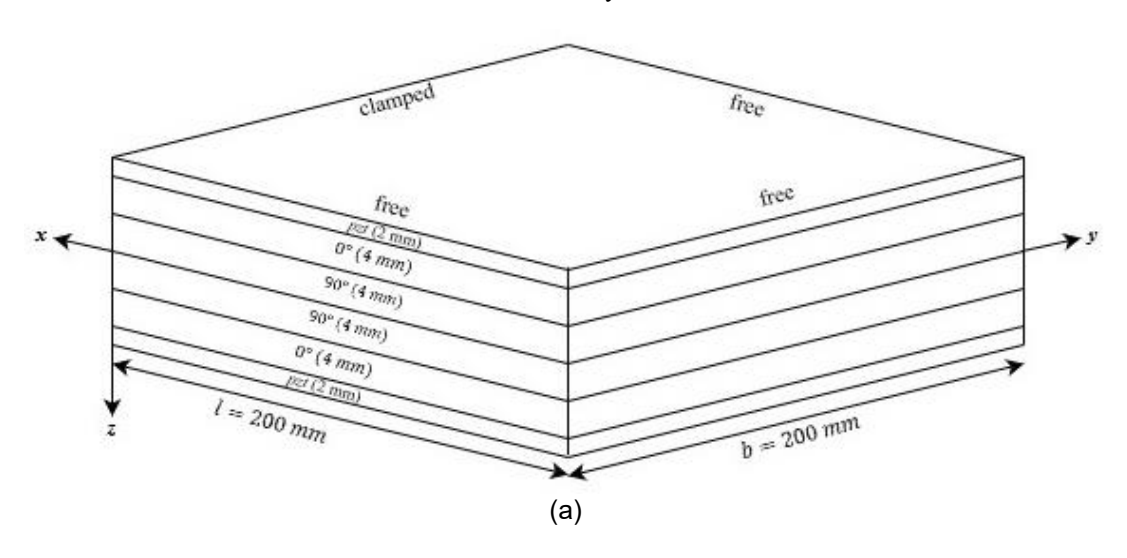
Figure 11 Variation of (a) central deflection, (b) Normal stress in Piezo-layer σ^p_{xx} (0.5a, 0.5b, 0.5b), (c) Normal stress in the Elastic layer σ^e_{xx} (0.5a, 0.5b, 0.4b) and (d) In-plane shear stress at the top layer $\tau_{xy}(a, 0.5b, 0.5b)$ for symmetric cross-ply laminates

Figure 11 illustrates the impact of incorporating higher-order non-linear coefficients on deflection, normal stresses, and in-plane stresses when a positive electric field is applied across the piezoelectric layers of a symmetric cross-ply laminate.

The results demonstrate that the inclusion of the elasto-striction coefficient enhances the accuracy of deflection and stress predictions. The elasto-striction coefficient significantly influences the bending stiffness, which decreases with a positive electric field and vice-versa. Additionally, the deflection and stress values are observed to be higher for symmetric cross-ply laminates compared to antisymmetric angle-ply laminates, attributed to the reduction in bending stiffness in the latter configuration.

3.4 Non-linear analysis of composite laminated plate under different end conditions

The effects of non-linear piezoelectric parameters are studied using an anti-symmetric angle-ply and symmetric cross-ply composite laminated plate with different end conditions as shown in Figure 12. The analysis considers a square piezoelectric composite laminated plate with a span length of 200 mm and a moderate thickness ratio of l/h = 10, consisting of four layers of graphiteepoxy substrate bonded to two outer layers of PZT APC (850) piezoceramic material with linear and non-linear material properties are listed in Table 1. The thickness of each composite layer is 4mm, while each piezoelectric layer has a thickness of 2 mm. The fibre orientation for the angle-ply and cross-ply laminates are $(p/-45^{\circ}/45^{\circ})_{as}$ and $(p/0^{\circ}/90^{\circ})_{s}$ and an electric field varying from 0 to 700 V/mm is applied across the top and bottom piezoelectric layers.



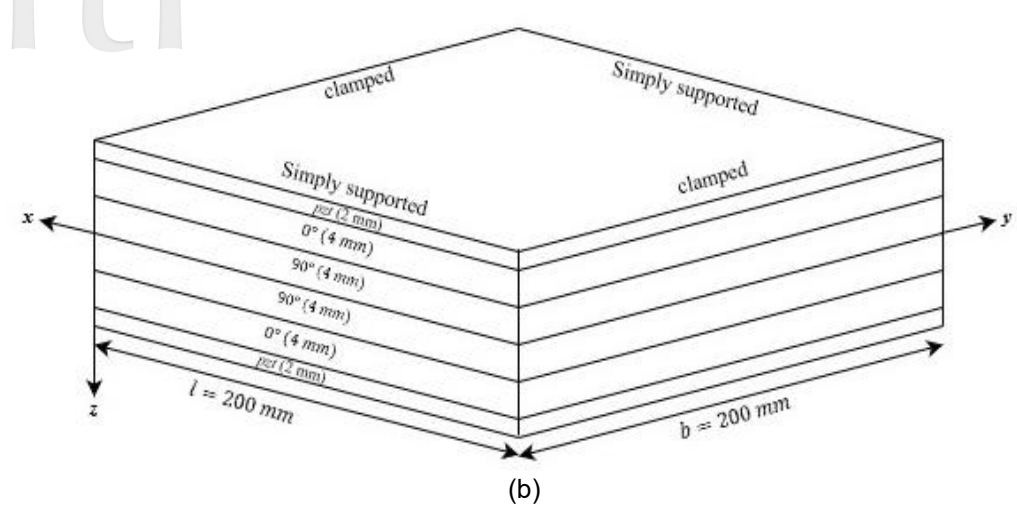


Figure 12 Symmetric cross-ply piezoelectric laminated composite plate with (a) cantilever end condition and (b) clamped simply supported end condition

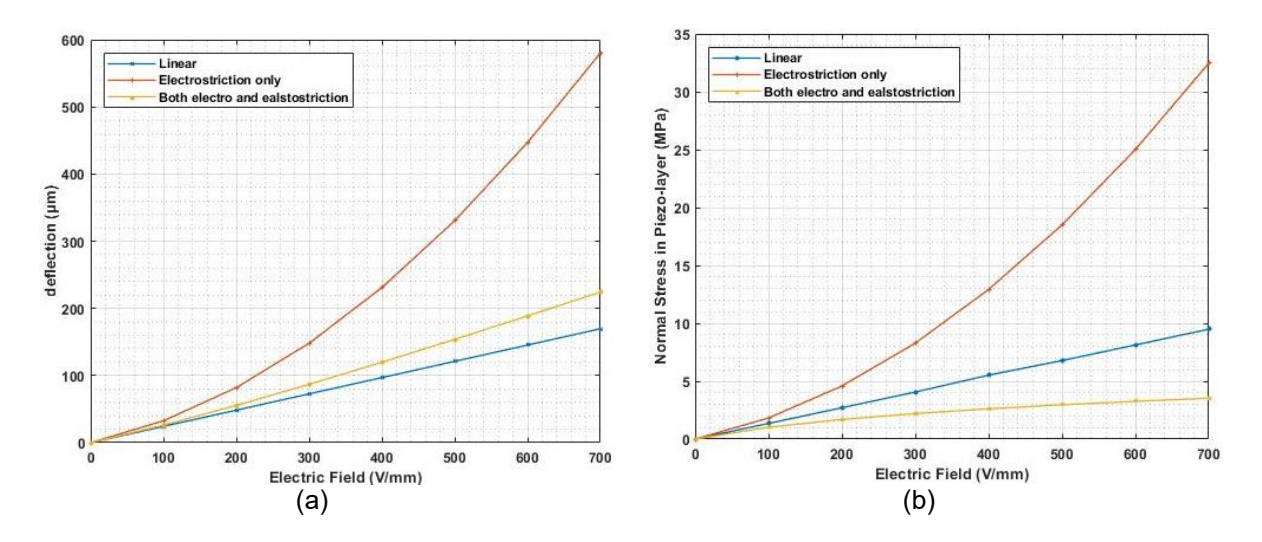


Figure 13 Variation of (a) transverse deflection at (a, 0.5b, 0), (b) Normal stress in Piezo-layer σ_{xx}^p (a, 0.5b, 0.5h), for cantilever anti-symmetric angle-ply piezoelectric laminate

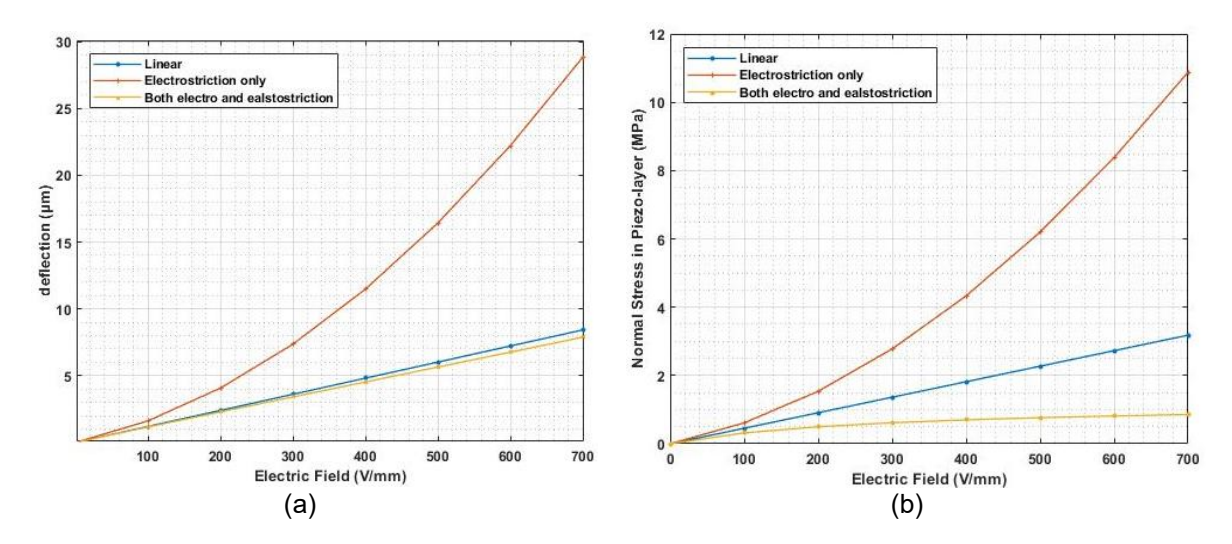


Figure 14 Variation of (a) transverse deflection at (0.5a, 0.5b, 0), (b) Normal stress in Piezo-layer σ_{xx}^p (0.5a, 0.5b, 0.5h), for clamped simply supported anti-symmetric angle-ply piezoelectric laminate

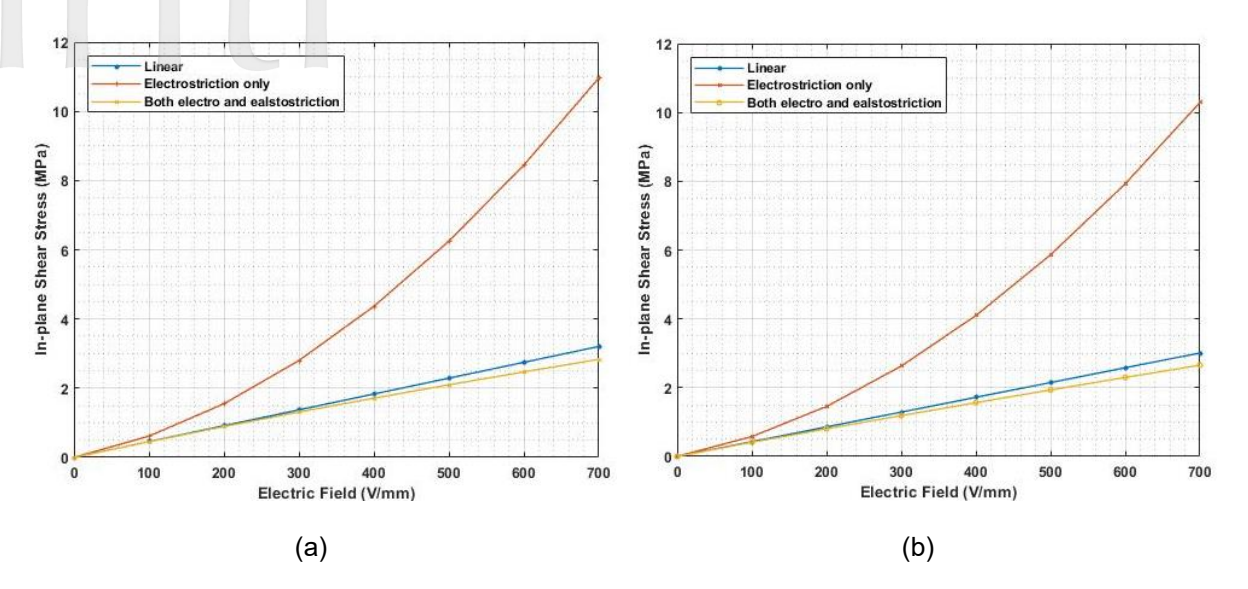


Figure 15 Variation of (a) In-plane shear stress at the top layer $\tau_{xy}(0,0.5b,0.5h)$ for cantilever antisymmetric angle-ply piezoelectric laminate, (b) In-plane shear stress at the top layer $\tau_{xy}(a,0.0.5h)$ for clamped simply supported anti-symmetric angle-ply piezoelectric laminate

The plot of deflection and stresses against varying electric fields is used to study effect of the non-linear terms. For anti-symmetric angle-ply, Figures 13, 14 and 15 presents the variation in transverse deflection, normal stress and in-plane shear stress under two boundary conditions: (a) a cantilever end condition (clamped at x = 0, with all other edges free) and (b) a clamped simply supported end condition (CSCS), where the edge at x = 0, t = 0 is clamped, and the remaining edges are simply supported along the t = 0-axis. Figures 16, 17 and 18 presents the variations in deflection, normal stress and in-plane shear stress for the symmetric cross-ply laminate configuration.

The results also reveal that the deflection is higher in an anti-symmetric angle-ply laminate with a cantilever end condition, due to the coupling between bending and extensional stiffness. In contrast, for more constrained boundary conditions, such as clamped or simply supported end conditions, the deflection is greater in cross-ply laminates. This difference arises because the piezoelectric actuation occurs along the ply orientation angle in cross-ply laminates, enhancing the deformation response. The comparison of deflection and stress plots for the two end conditions indicates that as the end conditions become more constrained, the plate becomes stiffer, which increases the impact of elasto-striction.

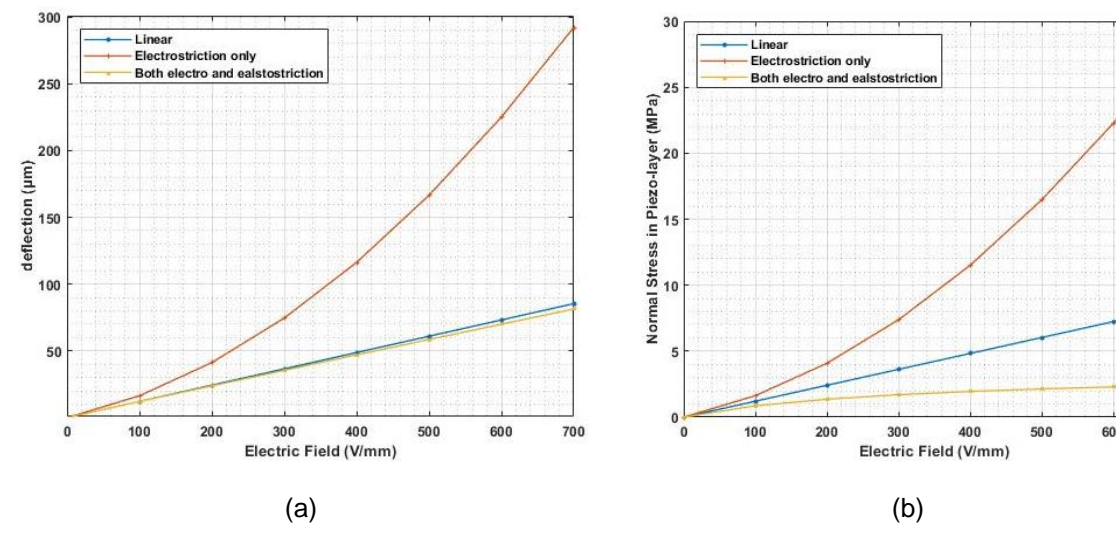


Figure 16 Variation of (a) transverse deflection at (a, 0.5b, 0), (b) Normal stress in Piezo-layer σ_{xx}^p (a, 0.5b, 0.5h), for cantilever symmetric cross-ply piezoelectric laminate

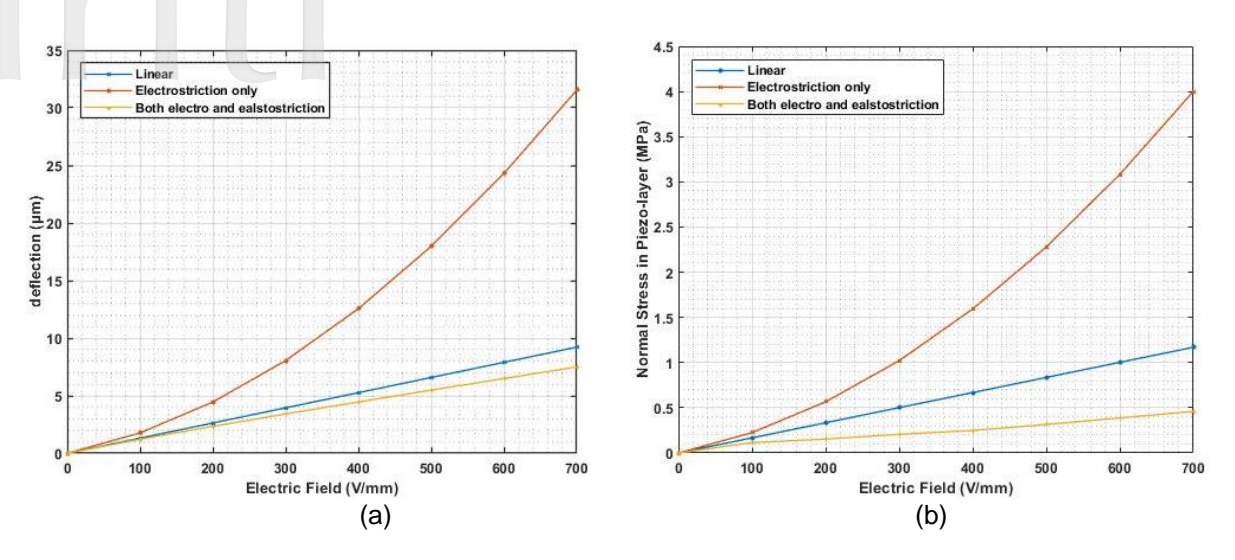


Figure 17 Variation of (a) transverse deflection at (0.5a, 0.5b, 0), (b) Normal stress in Piezo-layer σ_{xx}^p (0.5a, 0.5b, 0.5h), for clamped simply supported symmetric cross-ply piezoelectric laminate

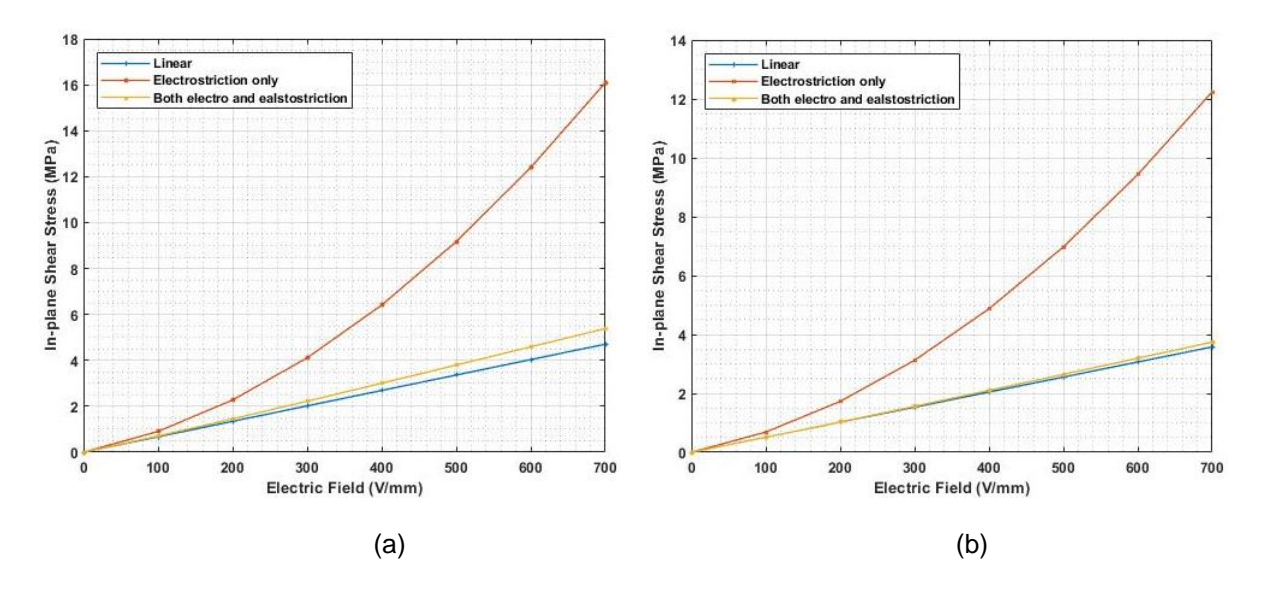


Figure 18 Variation of (a) In-plane shear stress at the top layer $\tau_{xy}(0,0.5b,0.5h)$ for cantilever symmetric cross-ply piezoelectric laminate, (b) In-plane shear stress at the top layer $\tau_{xy}(a,0,0.5h)$ for clamped simply supported symmetric cross-ply piezoelectric laminate

3.5 Deflection stress distribution of composite laminated plate along the thickness

To study the combined effect of considering both non-linear coefficients, an anti-symmetric angle-ply laminate and a cross-ply piezoelectric laminate with a length to thickness ratio of l/h=10 are considered. Applying an electric field of $700\,V/mm$, the distribution of longitudinal displacement, normal stress and in-plane shear stress along the thickness of the plate is plotted in Figure 19. The figure shows the difference in linear and non-linear response of displacement and stresses. The distribution of non-linear normal stress reveals significantly lower stress values in the piezoelectric

layer due to the reduction in elastic properties influenced by the elasto-striction coefficient, while slightly higher values of normal stresses are obtained in composite ply due to higher values of deflection in laminates. The coupling between transformed extensional and bending stiffness leads to higher deflection and stress values in the antisymmetric laminate compared to the cross-ply configuration. Additionally, the difference in inplane shear stress distribution between the linear and non-linear piezoelectric constitutive equations is more pronounced in the piezoelectric layer, as the deflection variation increases with the distance from the mid-plane.

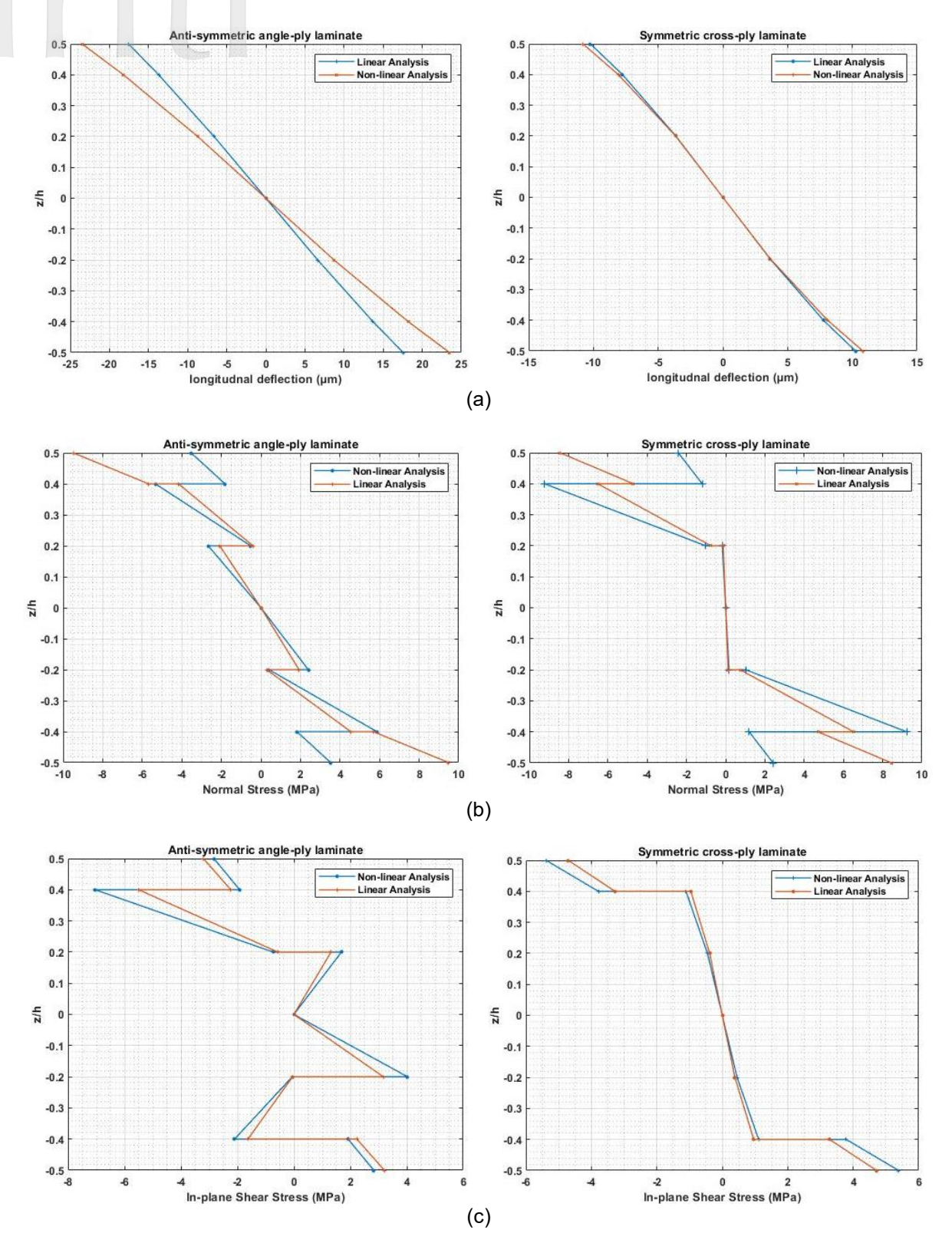


Figure 19 Linear and non-linear response across thickness for cantilever anti-symmetric angle-ply and symmetric cross-ply laminate (a) longitudinal deflection distribution i.e. $u_x(a, 0.5b, z)$, (b) Normal stress distribution i.e. σ_{xx} (a, 0.5b, z), (c) In-plane shear stress distribution i.e. $\tau_{xy}(0.0.5b, z)$

IV. CONCLUSIONS

The paper investigates the impact of incorporating higher-order non-linear terms in the

constitutive equation of a piezoelectric actuator on the static analysis of a composite laminated plate, utilizing a finite element model based on higherorder shear deformation theory. The finite element model is validated by comparing the results for composite laminates under both linear and nonlinear constitutive equations, using cantilever and simply supported bimorph as well as uni-morph configurations. Results of static analysis of the plate are presented to show the effect of considering electro-striction and elasto-striction coefficients. The effect of considering a higher-order non-linear piezoelectric coefficient is analyzed through examples with varying laminate orientation and end conditions. The findings indicate that the inclusion of the non-linear coefficients is important at high electric fields, as linear constitutive equations fail to accurately predict the deflection and stress responses. The inclusion of the elasto-striction coefficient influences the elastic properties of the piezoelectric layers, leading to a reduction in deflection and stresses in composite laminates. In contrast, the electro-striction coefficient results in significantly higher values of deflection and stresses. When both non-linear coefficients are considered, the deflection and stresses in the non-piezo composite layer increase with the electric field, compared to the linear deflection and stresses, whereas in the piezoelectric layer, normal stresses decrease due to a reduction in the elastic properties of the piezoelectric material at high electric fields. Higher deflection and stresses are observed in antisymmetric angle-ply laminates compared to symmetric cross-ply laminates under cantilever end conditions, due to the coupling between extension and bending stiffness. However, when the end conditions are constrained, symmetric cross-ply laminates exhibit more deflection than antisymmetric angle-ply laminates, as the actuation in the piezoelectric layer occurs along the ply orientation angle. The results of static analysis of the piezoelectric actuated composite laminated plate show that non-linear piezoelectric coefficients cannot be ignored. The use of non-linear coefficients can be further analyzed for vibration and dynamic control of piezoelectric laminates with different orientations and end conditions.

REFERENCES

- [1] Khosravani M R, Anders D and Weinberg K, "Influence of strain rate on fracture behavior of sandwich composite T-joints," *European Journal of Mechanics A/Solids*, Vol. 78, 2019, pp. 103821. https://doi.org/10.1016/j.euromechsol.2019.1 03821
- [2] Liew KM, Pan ZZ, Zhang LW, "An overview of layerwise theories for composite laminates and structures: Development, numerical implementation and application," *Composite Structures*, Vol. 216, 2019, pp. 240-59.

- https://doi.org/10.1016/j.compstruct.2019.02.
- [3] Kuo SY, "Design and Buckling Analysis of Fully Functionally Graded Carbon Nanotube Reinforced Hybrid Composite Laminates," *Journal of Aeronautics, Astronautics and Aviation*, Vol. 50, No. 2, 2018, pp. 121-134. https://doi.org/10.6125/JoAAA.201806-50(2">https://doi.org/10.6125/JoAAA.201806-50(2">https://doi.org/10.6125/JoAAA.201806-50(2">https://doi.org/10.6125/JoAAA.201806-50(2">https://doi.org/10.6125/JoAAA.201806-50(2">https://doi.org/10.6125/JoAAA.201806-50(2">https://doi.org/10.6125/JoAAA.201806-50(2">https://doi.org/10.6125/JoAAA.201806-50(2")
- [4] Van Nguyen T, Hwu C, "A Review on Modelling Polymer Composites via Anisotropic Viscoelasticity," *Journal of Aeronautics, Astronautics and Aviation*, Vol. 53, No. 3, 2021, pp. 387-402. https://doi.org/10.6125/JoAAA.202109_53(3">https://doi.org/10.6125/JoAAA.202109_53(3">https://doi.org/10.6125/JoAAA.202109_53(3").05
- [5] Zhang M, Sun B, Gu B, "Meso-structure ageing mechanism of 3-D braided composite's compressive behaviors under accelerated thermo-oxidative ageing environment," *Mechanics of Materials*, Vol. 115, 2017, pp. 47-63.

 https://doi.org/10.1016/j.mechmat.2017.09.0
 02
- [6] Adnan Elshafei M, Farid A,Omer AA, "Modeling of torsion actuation of beams using inclined piezoelectric actuators," *Archive of Applied Mechanics*, Vol. 85, 2015, pp. 171-189.
 - https://doi.org/10.1007/s00419-014-0910-6
- [7] Gohari S, Mozafari F, Moslemi N, Mouloodi S, Sharifi S, Rahmanpanah H, Burvill C, "Analytical solution of the electro-mechanical flexural coupling between piezoelectric actuators and flexible-spring boundary structure in smart composite plates," *Archives of Civil and Mechanical*, Vol. 21, No. 33, 2021.
 - https://doi.org/10.1007/s43452-021-00180-z
- [8] Wang QM, Zhang Q, Xu B, Liu R, Cross L E, "Nonlinear piezoelectric behavior of ceramic bending mode actuators under strong electric fields," *Journal of Applied Physics*, Vol. 86, 1999, pp. 3352-3360.
 - https://doi.org/10.1063/1.371213
- [9] Chee CYK, Tong L, Steven GP, "A Review on the Modelling of Piezoelectric Sensors and Actuators Incorporated in Intelligent Structures," Journal of Intelligent Material Systems and Structures, Vol. 9, No. 1, 1998, pp. 3-19.

- https://doi.org/10.1177/1045389X980090010
- [10] Rao SS, Sunar M, "Piezoelectricity and its use in disturbance sensing and control of flexible structures: a survey," *Applied Mechanics*, Vol. 47, No. 4, 1994, pp. 113-123. https://doi.org/10.1115/1.3111074
- [11] Masys AJ, Ren W, Yang G, Mukherjee BK, "Piezoelectric strain in lead zirconate titante ceramics as a function of electric field, frequency, and dc bias," *Journal of Applied Physics*, Vol. 94, 2003, pp. 1155-1162. https://doi.org/10.1063/1.1587008
- [12] Kugel VD, Cross LE, "Behavior of soft piezoelectric ceramics under high sinusoidal electric fields," *Journal of Applied Physics*, Vol. 84, No. 5, 1998, pp. 2815-2830. https://doi.org/10.1063/1.368422
- [13] Mueller V, Fuchs E, Beige H, "Characterization of nonlinear properties of soft PZT-piezoceramics," Ferroelectrics, Vol. 240, No. 1, 2000, pp. 1333-1340. https://doi.org/10.1080/00150190008227954
- [14] Zhang QM, Wang H, Zhao J, "Effect of Driving Field and Temperature on the Response Behavior of Ferroelectric Actuator and Sensor Materials," *Journal of Intelligent Material Systems and Structures Struct.*, Vol. 6, No. 1, 1995, pp. 84-93. https://doi.org/10.1177/1045389X950060011
- [15] Priya S, Viehland D, Carazo AV, Ryu J, Uchino K, "High-power resonant measurements of piezoelectric materials: Importance of elastic nonlinearities," *Journal* of Applied Physics, Vol. 90, No. 3, 2001, pp. 1469-1479.

https://doi.org/10.1063/1.1381046

- [16] Bruno BP, Fahmy AR, Stürmer M, Wallrabe U, Wapler MC, "Properties of piezoceramic materials in high electric field actuator applications," *Smart Materials and Structures*, Vol. 28, No. 1, 2018, pp. 15029.
 https://doi.org/10.1088/1361.665X/2008fb
 - https://doi.org/10.1088/1361-665X/aae8fb
- [17] Yao LQ, Zhang JG, Lu L, Lai MO, "Nonlinear static characteristics of piezoelectric bending actuators under strong applied electric field," *Sensors and Actuators A: Physical*, Vol. 115, No. 1, 2004, pp. 168-175.
 - https://doi.org/10.1016/j.sna.2004.04.037
- [18] Thornburgh RP, Chattopadhyay A, "Nonlinear actuation of smart composites

- using a coupled piezoelectric mechanical model," *Smart Materials and Structures*, Vol. 10, No. 4, 2001, pp. 743-749. https://doi.org/10.1088/0964-1726/10/4/319
- [19] Wischke M, Haller D, Goldschmidtboeing F, Woias P, "Assessing the elastostriction and the electrostriction parameter of bulk PZT ceramics," Smart Materials and Structures, Vol. 19, No. 8, 2010. https://doi.org/10.1088/0964-1726/19/8/085003
- [20] Joshi SP, "Non-linear constitutive relations for piezoceramic materials," *Smart Materials and Structures*, Vol. 1, No. 1, 1992, pp. 80-83. https://doi.org/10.1088/0964-1726/1/1/012
- [21] Arafa M, Baz A, "On the Nonlinear Behavior of Piezoelectric Actuators," *Journal of Vibration and Control*, Vol. 10, No. 3, 2004, pp. 387-398.

 https://doi.org/10.1177/1077546304033365
- [22] Tiersten HF, "Electroelastic equations for electroded thin plates subject to large driving voltages," *Journal of Applied Physics*, Vol. 74, No. 5, 1993, pp. 3389-3393. https://doi.org/10.1063/1.354565
- [23] Chattaraj N, Ganguli R, "Electromechanical analysis of piezoelectric bimorph actuator in static state considering the nonlinearity at high electric field," *Mechanics of Advanced Materials and Structures*, Vol. 23, No. 7, 2016, pp. 802-810. https://doi.org/10.1080/15376494.2015.1029 168
- [24] Chattaraj N, Ganguli R, "Effect of selfinduced electric displacement field on the response of a piezo-bimorph actuator at high electric field," *International Journal of Mechanical Sciences*, Vol. 120, 2017, pp. 341-348. https://doi.org/10.1016/j.ijmecsci.2016.11.01
- [25] Chattaraj N, Ganguli R, "Performance improvement of a piezoelectric bimorph actuator by tailoring geometry," *Mechanics of Advanced Materials and Structures*, Vol. 25, No. 10, 2018, 829-835.

 https://doi.org/10.1080/15376494.2017.1308
 590
- [26] Ahoor ZH, Ghafarirad H, Zareinejad M, "Nonlinear dynamic modeling of bimorph piezoelectric actuators using modified constitutive equations caused by material

nonlinearity," Mechanics of Advanced Materials and Structures, Vol. 28, No. 8, 2019, pp. 763-773.

Mohd Sultan Ibrahim Shaik Dawood

https://doi.org/10.1080/15376494.2019.1590 885

[27] Liu GR, Dai KY, Lim KM, "Static and vibration control of composite laminates integrated with piezoelectric sensors and actuators using the radial point interpolation method," Smart Materials and Structures, Vol. 13, No. 6, 2004, pp. 1438-1447.

https://doi.org/10.1088/0964-1726/13/6/015

[28] Phung-Van P, Nguyen-Thoi T, Le-Dinh T, Nguyen-Xuan H, "Static and free vibration analyses and dynamic control of composite plates integrated with piezoelectric sensors and actuators by the cell-based smoothed discrete shear gap method (CS-FEM-DSG3)," Smart Materials and Structures, Vol. 22, No. 9, 2013.

> https://doi.org/10.1088/0964-1726/22/9/095026

[29] Kapuria S, Yasin MY, "A nonlinear efficient layerwise finite element model for smart piezolaminated composites under strong applied electric field," Smart Materials and Structures, Vol. 22, No. 5, 2013.

https://doi.org/10.1088/0964-1726/22/5/055021

[30] Yaqoob Yasin M, Kapuria S, "Influence of piezoelectric nonlinearity on active vibration suppression of smart laminated shells using strong field actuation," Journal of Vibration and Control, Vol. 24, No. 3, 2016, pp. 505-

https://doi.org/10.1177/1077546316645220

[31] Kapuria S, Yasin MY, Hagedorn P, "Active vibration control of piezolaminated composite plates considering strong electric field nonlinearity," AIAA Journal, Vol. 53, No. 3, 2015, pp. 603-616.

https://doi.org/10.2514/1.J053166

[32] Rao MN, Tarun S, Schmidt R, Schröder KU, "Finite element modeling and analysis of piezo-integrated composite structures under large applied electric fields," Smart Materials and Structures, Vol. 25, 2016. https://doi.org/10.1088/0964-

1726/25/5/055044

[33] Zhang SQ, Zhao GZ, Zhang SY, Schmidt R and Qin X S, "Geometrically nonlinear FE analysis of piezoelectric laminated composite structures under strong driving electric field," Composite Structures, Vol. 181, 2017, pp. 112-120.

https://doi.org/10.1016/j.compstruct.2017.08. 052

- [34] Sumit Kane SR, Sinha AK, Shukla R, "Electric field-induced nonlinear behavior of lead zirconate titanate piezoceramic actuators in bending mode," Mechanics of Advanced Materials and Structures, Vol. 30, No. 10, 2022, pp. 2111-2120. https://doi.org/10.1080/15376494.2022.2050
- [35] Sumit Kane SR, Sinha AK, Ganguli T, Shukla R, "Iterative piezo response function-based optimization for static shape control of cantilever beam using nonlinear piezoactuators," Smart Materials Structures, Vol. 32, No. 1, 2022. https://doi.org/10.1088/1361-665X/aca4ae
- [36] Sumit RS, Sinha AK, Kane SR, "Response of piezoelectric ceramic actuator under high electric field in bending mode," AIP Conference Proceedings, Vol. 2648, No. 1,

https://doi.org/10.1063/5.0114401

[37] Akhlaq A, Dawood MSIS, Syed MAJ, Sulaeman E, "A Study on the Effect of Piezoelectric Nonlinearity on the Bending Behaviour of Smart Laminated Composite Beam," Materials (Basel). Vol. 16, No. 7,

https://doi.org/10.3390/ma16072839

[38] Reddy JN, "A simple higher-order theory for laminated composite plates," Journal of Applied Mechanics, Vol. 51, No. 4, 1984, pp. 745-752.

https://doi.org/10.1115/1.3167719

[39] Shen NH, "Analysis of beams containing piezoelectric sensors and actuators," Smart Materials and Structures, Vol. 3, No. 4, 1994, pp. 439-447.

https://doi.org/10.1088/0964-1726/3/4/006

- [40] Lam KY, Peng X Q, Liu GR, Reddy JN, "A finite-element model for piezoelectric composite laminates," Smart Materials and Structures, Vol. 6, No. 5, 1997, pp. 583-591. https://doi.org/10.1088/0964-1726/6/5/009
- [41] Yao LQ, Zhang JG, Lu L, Lai MO, "Nonlinear extension and bending of piezoelectric laminated plate under large applied field

21

actuation," *Smart Materials and Structures*, Vol. 13, No. 2, 2004, pp. 404-414. https://doi.org/10.1088/0964-1726/13/2/019